

## Subtlety of the Structure—Affinity and Structure—Efficacy Relationships around a Nonpeptide Oxytocin Receptor Agonist

Marie-Céline Frantz,<sup>†,§</sup> Jordi Rodrigo,<sup>†,||</sup> Laure Boudier,<sup>‡</sup> Thierry Durroux,<sup>‡</sup> Bernard Mouillac,<sup>‡</sup> and Marcel Hibert<sup>\*,†</sup>

<sup>†</sup>Laboratoire d'Innovation Thérapeutique, UMR 7200 CNRS/Université de Strasbourg, Faculté de Pharmacie, 74 route du Rhin, BP60024, 67401 Illkirch, France and <sup>‡</sup>Institut de Génomique Fonctionnelle UMR CNRS 5203/INSERM U661/Université Montpellier I & II, Dept Pharmacologie Moléculaire, 141 rue de la Cardonille, 34094 Montpellier, France. <sup>§</sup>Current address: University of Pittsburgh, Department of Chemistry, Pittsburgh, Pennsylvania 15260. <sup>||</sup>Current address: Université Paris-Sud, CNRS, BioCIS-UMR 8076, Laboratoire de Chimie Thérapeutique, Faculté de Pharmacie, 5 rue J.-B. Clément, 92296 Châtenay-Malabry, France

Received July 22, 2009

Very few nonpeptide oxytocin agonists have currently been reported, and none of them seem suitable for the *in vivo* investigation of the oxytocin mediated functions. In an attempt to rationalize the design of better tools, we have systematically studied the structural determinants of the affinity and efficacy of representative ligands of the V<sub>1a</sub>, V<sub>2</sub>, and OT receptor subtypes. Despite apparently obvious similarity between the ligand structures on one hand, and between the receptor subtypes on the other hand, the binding affinity and the functional activity profiles of truncated and hybrid ligands highlight the subtlety of ligand–receptor interactions for obtaining nonpeptide OT receptor agonists.

### Introduction

Numerous animal studies have provided evidence supporting a role for oxytocin (OT<sup>9</sup>) and vasopressin (AVP) in many central nervous system (CNS) functions including mating, affiliation, adult pairing and faithfulness, anxiety, and prosocial behaviors.<sup>1–6</sup> In humans, OT has been reported to improve trust<sup>7–9</sup> and to decrease fear associated to social phobia<sup>10–12</sup> and symptoms related to autism.<sup>13–20</sup> However, the only molecular probe that is currently available to study these functions, both in animals (usually after intracerebroventricular administration) and humans (after intranasal administration), is oxytocin itself or closely related peptide analogues that have a poor bioavailability inherent with most neuropeptides (e.g., poor intestinal and blood–brain barrier penetration, short half-life, rapid clearance). To characterize without ambiguity the different central mechanisms of action and physiopathological functions of vasopressin and oxytocin,

there was an urgent need for centrally active, potent, specific, and bioavailable agonists and antagonists of the four vasopressin and oxytocin receptor subtypes, namely the V<sub>1a</sub>, V<sub>1b</sub>, V<sub>2</sub>, and OT receptors. Such antagonists became recently available.<sup>21</sup> However, very few nonpeptide agonists have been reported.<sup>22</sup> For OT receptor agonists, the most interesting to date (compound **1**, Figure 1) is the optimized analogue of a hit discovered by systematic screening.<sup>23,24</sup> However, its structure does not seem optimal for CNS *in vivo* studies because its molecular weight (MW = 600.8 Da) and its number of H-bonds (14 H-bonds possible) remain rather high.<sup>25</sup> In addition, some of its hydrophobicity parameters do not fit the requirements for a significant blood–brain barrier penetration (ideal clogP = 2 but high PSA = 121 Å<sup>2</sup>). Furthermore, its efficacy and selectivity profile had to be further explored. We have used this molecule and closely related analogues acting at other vasopressin receptor subtypes to systematically explore the structural determinants of affinity, efficacy, and selectivity at V<sub>1a</sub>, V<sub>2</sub>, and OT receptor subtypes. Our strategy consisted in two steps. First, we tried to dissect compound **1** to identify the minimum molecular components required for affinity and to evaluate their positive (agonism) or negative (antagonism) contribution to efficacy on the three considered receptor subtypes. To this end, truncated analogues were prepared and their affinity and efficacy were measured in parallel on the target receptors. Second, we systematically prepared hybrid molecules combining the apparently homologous molecular fragments of four representative vasopressin/oxytocin ligands (Table 1): compound **1**, a claimed OT receptor agonist;<sup>24</sup> compound **2**, a reported nonselective V<sub>1a</sub>/V<sub>2</sub>/OT receptor antagonist;<sup>26</sup> compound **3**, WAY-VNA-932, a V<sub>2</sub> receptor agonist;<sup>27</sup> and compound **4**, L-371,257, the structurally closest and selective OT receptor antagonist.<sup>28</sup> The affinity and efficacy of these chimeric molecules for the V<sub>1a</sub>, V<sub>2</sub>, and OT receptor subtypes were studied to probe the contribution to

\*To whom correspondence should be addressed. Phone: +33390244232. Fax: +33390244310. E-mail: mhibert@pharma.u-strasbg.fr.

<sup>9</sup>Abbreviations: AVP, arginine vasopressin; BSA, bovine serum albumin; cAMP, cyclic adenosine 5'-monophosphate; CDI, carbonyl-diimidazole; CHO, Chinese hamster ovary; CNS, central nervous system; CRE, cAMP response element; DCM, dichloromethane; DIEA, diisopropylethylamine; DMAP, *N,N*-dimethyl-4-aminopyridine; D-MEM, Dulbecco's modified Eagle's medium; DMF, dimethylformamide; DMSO, dimethylsulfoxide; E, extracellular loop; EDCl, 1-(3-dimethylaminopropyl)-3-ethyl-carbodiimide; EDTA, ethylenediamine-tetraacetic acid; GPCR, G protein-coupled receptor; HOBt, *N*-hydroxybenzotriazole; IP<sub>1</sub>, *myo*-inositol 1-phosphate;  $\mu$ w, microwaves; NFAT, nuclear factor of activated T-cells; NMP, *N*-methyl-2-pyrrolidone; OT, oxytocin; OT-R, oxytocin receptor; Ro-20-1724, 4-(3-butoxy-4-methoxyphenyl)methyl-2-imidazolidone; rt, room temperature; SAR, structure–activity relationships; SEM, standard error of the mean; TFA, trifluoroacetic acid; THF, tetrahydrofuran; TM, transmembrane domain; Tris, 2-amino-2-hydroxymethyl-1,3-propanediol; V<sub>1a</sub>-R, vasopressin V<sub>1a</sub> receptor subtype; V<sub>1b</sub>-R, vasopressin V<sub>1b</sub> receptor subtype; V<sub>2</sub>-R, vasopressin V<sub>2</sub> receptor subtype.

affinity and efficacy of the different corresponding fragments. The unexpected results shed an interesting and disturbing light on the mode of action of very similar ligands on very similar receptor subtypes.

## Chemistry

Reference compounds **2**, **3**, and **4** were prepared according to literature protocols.<sup>26–28</sup> Compound **1** and analogues **12a–c** were prepared according to Scheme 1. The general procedure is similar to the synthesis previously described by Pitt et al.<sup>24,29</sup> with some optimization, specifically for the cyclization step leading to the lactam **6**. The original preparation consisting of reflux in

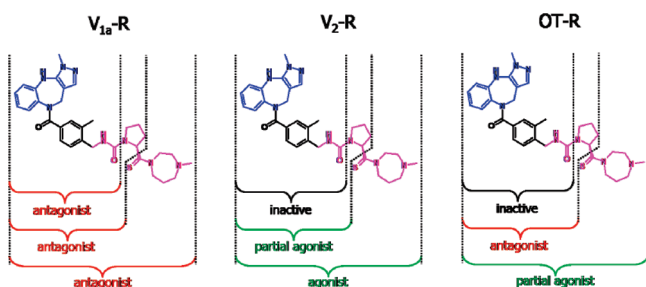


**Figure 1.** Schematic representation of the main results of the truncated analogues of compound **1**.

isopropyl alcohol for 14 days in the presence of acetic acid was difficult to reproduce. However, a 89% yield could be achieved by heating the precursor **5** in a sealed tube at 160 °C for 48 h. As described for compound **1**, the urea truncated analogues **12a** and **12b** could be isolated in high yields after coupling with the common amine intermediate **10** via preactivation with carbonyldiimidazole (CDI). Alternatively, the acetylated truncated analogue **12c** was obtained by reacting **10** with acetic anhydride.

A similar synthetic route was followed for the preparation of compounds **23a–d**, according to the general Scheme 2. The polycyclic amines **13**, **14**, and **15** were prepared according to literature protocols.<sup>30–32</sup> In addition, with regard to the synthesis of the analogue **23c**, the key acid intermediate **20** was prepared starting from the acyl chloride **16** via a Sandmeyer reaction to introduce the nitrile group.

As described in Scheme 3, the hybrid compound **27** was prepared in a similar manner as the reference compound **2**. Finally, both hybrids **31a** and **31b** were obtained following a general route described by Kondo et al.<sup>33</sup>

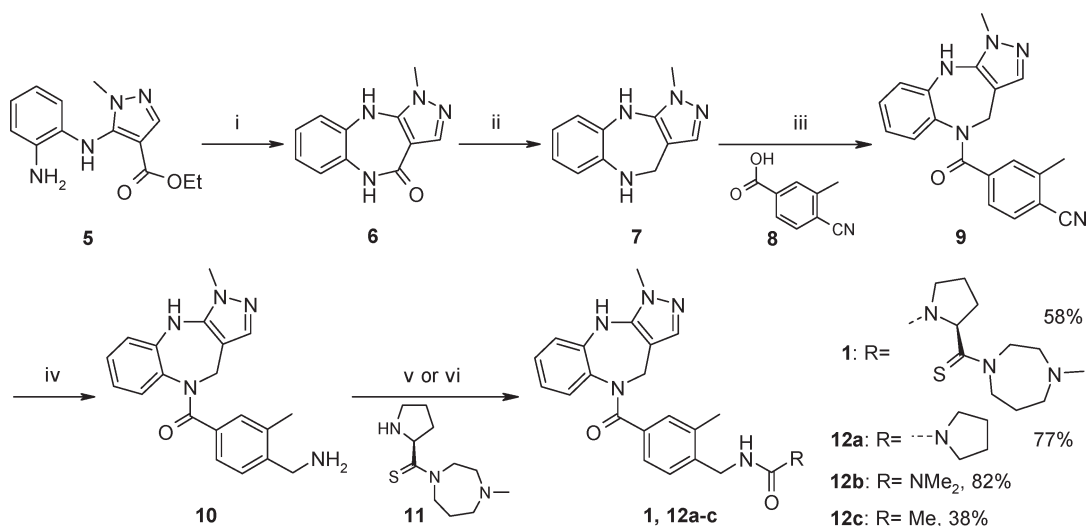
## Biology

The affinities of the different ligands for the human vasopressin receptors subtypes and the oxytocin receptor were determined on CHO cell membranes by competition experiments against [<sup>3</sup>H]AVP, as described previously.<sup>34–36</sup>

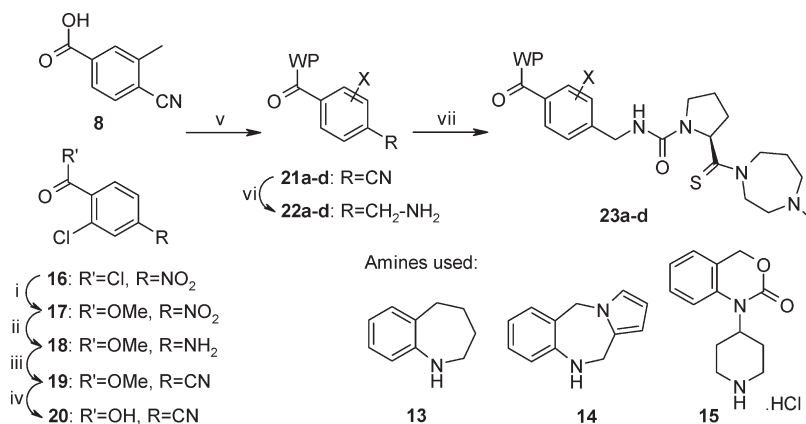
**Table 1.** Structures and Biological Activities of the Reference Compounds<sup>g</sup>

cpd	structure	OT-R			V <sub>1a</sub> -R			V <sub>2</sub> -R		
		K <sub>i</sub> <sup>a</sup>	K <sub>act</sub> <sup>b</sup>	K <sub>inact</sub> <sup>c</sup>	K <sub>i</sub> <sup>a</sup>	K <sub>act</sub> <sup>b</sup>	K <sub>inact</sub> <sup>c</sup>	K <sub>i</sub> <sup>a</sup>	K <sub>act</sub> <sup>b</sup>	K <sub>inact</sub> <sup>c</sup>
<b>1</b>		147 ± 11	667 ± 68 58 ± 2%	16 ± 6%	330 ± 38	ns	271 ± 61	>1000	599 ± 91 84 ± 4%	ns
<b>2</b>		63 <sup>26</sup>	ns	171 ± 29	14 <sup>26</sup>	ns	63 ± 8	7.6 <sup>26</sup>	0.57 ± 0.18	0.096 ± 0.030
<b>3</b> WAY-VNA-932		125 <sup>27</sup>	ns	488 ± 147	465 <sup>27</sup>	ns	33 ± 3%	39.9 <sup>27</sup>	50 ± 4	9.5 ± 3.1 75 ± 8%
<b>4</b> L-371,257		4.6 <sup>28</sup>	ns <sup>e</sup>	0.93 ± 0.10 <sup>f</sup>	3200 <sup>28</sup>	ns <sup>e</sup>	18% <sup>e</sup>	37000 <sup>28</sup>	nd <sup>d</sup>	ns <sup>e</sup>

<sup>a</sup> The inhibition constants (K<sub>i</sub> in nM) for human V<sub>1a</sub>, V<sub>2</sub>, and OT receptors were determined on CHO cell membranes by competition binding assays (displacement of radioactive [<sup>3</sup>H]AVP). Results are expressed as mean ± SEM of at least three separate experiments performed in triplicate. When K<sub>i</sub> > 1000 nM, these are results of at least two separate experiments performed in triplicate. <sup>b</sup> The activation constants (K<sub>act</sub> in nM) were measured in CHO cell lines expressing either vasopressin V<sub>1a</sub> or V<sub>2</sub> or oxytocin receptor by IP-One (V<sub>1a</sub>-R and OT-R, IP<sub>1</sub> accumulation) or cAMP dynamic 2 (V<sub>2</sub>-R, cAMP accumulation) assays. These values are the mean ± SEM of at least three separate experiments performed in triplicate. The maximal stimulations (E<sub>max</sub>) are expressed as percentages of the endogenous agonist maximal stimulation at [ligand] = 1 μM (n = 3). In case of a weak stimulation, results are expressed as percentages of the endogenous agonist maximal stimulation at [ligand] = 1 μM (n = 2). Results are not significant (ns) when there is < 10% response at [ligand] = 1 μM (n = 2). <sup>c</sup> The inactivation constants (K<sub>inact</sub> in nM) were measured in CHO cell lines expressing either vasopressin V<sub>1a</sub> or V<sub>2</sub> or oxytocin receptor by IP-One (V<sub>1a</sub>-R and OT-R, inhibition of agonist-induced IP<sub>1</sub> accumulation) or cAMP dynamic 2 (V<sub>2</sub>-R, inhibition of agonist-induced cAMP accumulation) assays. These values are the mean ± SEM of at least three separate experiments performed in triplicate. In case of a weak inhibition, results are expressed as percentages of endogenous agonist-response inhibition at [ligand] = 1 μM (n = 2). Results are not significant (ns) when there is < 10% response inhibition at [ligand] = 1 μM (n = 2). <sup>d</sup> Not determined. <sup>e</sup> n = 1, <sup>f</sup> n = 2. <sup>g</sup> Putatively homologous binding components are displayed with similar colors. **1** is a claimed OT receptor agonist;<sup>23,24</sup> **2** is a nonselective V<sub>1a</sub>/V<sub>2</sub>/OT receptor antagonist;<sup>26</sup> **3**, WAY-VNA-932, is a V<sub>2</sub> receptor agonist;<sup>27</sup> **4**, L-371,257, is a selective OT receptor antagonist.<sup>28</sup>

**Scheme 1.** Synthesis of Compound **1** and Truncated Analogues<sup>a</sup>

<sup>a</sup> Reagents and conditions: (i) 1:9 AcOH/*i*PrOH, sealed flask, 160 °C, 48 h, 89%. (ii) LiAlH<sub>4</sub>, THF, reflux, 44 h, 86%. (iii) (a) **8**, (COCl)<sub>2</sub>, cat. DMF, DCM, 2 h; (b) **7**, Et<sub>3</sub>N, DCM, 2 d, 75%. (iv) NaBH<sub>4</sub>, CoCl<sub>2</sub>·6H<sub>2</sub>O, MeOH, 1 h, quant. (v) (a) CDI, DIEA, DMF, 1 h; (b) **11** or pyrrolidine or Me<sub>2</sub>NH·HCl, DIEA, DMF, overnight, 58–82%. (vi) Ac<sub>2</sub>O, Et<sub>3</sub>N, DCM, 3 h, 38%.

**Scheme 2.** Synthesis of the Molecular Hybrids Conserving the Eastern Part of Compound **1**<sup>a</sup>

<sup>a</sup> Reagents and conditions: (i) MeOH, 2 h, quant. (ii) SnCl<sub>2</sub>·2H<sub>2</sub>O, EtOH, reflux, 1 h, quant. (iii) (a) NaNO<sub>2</sub>, conc HCl/H<sub>2</sub>O, -15 °C, 15 min; (b) CuCN, KCN, H<sub>2</sub>O, -10 °C–rt, 2 h, 61%. (iv) LiOH·H<sub>2</sub>O, MeOH/THF, 1 h, 83%. (v) For **21a**: (a) **8**, (COCl)<sub>2</sub>, cat. DMF, DCM, 1 h; (b) **13**, pyridine, cat. DMAP, DCM, overnight, 76%; for **21b**: (a) **8**, (COCl)<sub>2</sub>, cat. DMF, DCM, 1 h; (b) **14**, pyridine, DCM, 1 h, 65%; for **21c**: (a) **20**, (COCl)<sub>2</sub>, cat. DMF, DCM, 0 °C, 1 h; (b) **14**, pyridine, cat. DMAP, DCM, μw 80 °C, 6 min, 49%; for **21d**: **8**, **15**, HOBT·H<sub>2</sub>O, EDCI·HCl, DIEA, DMF, 14 h, 65%. (vi) NaBH<sub>4</sub>, CoCl<sub>2</sub>·6H<sub>2</sub>O, MeOH, 1–3 h, 12–89%. (vii) (a) CDI, DIEA, DMF, 1–3 h; (b) **11**, DIEA, DMF, 16–40 h, 51–95%.

The functional agonist and competitive antagonist properties of each ligand were determined for the human vasopressin and oxytocin receptors subtypes stably expressed in CHO cells. The accumulation of *myo*-inositol 1-phosphate (V<sub>1a</sub> and OT receptors) was determined by the IP-One assay and the accumulation of cAMP (V<sub>2</sub> receptor) was determined by the cAMP *dynamic 2* assay, both kindly provided by Cisbio International. These immunoassays are based on the competition between free IP<sub>1</sub> or cAMP and IP<sub>1</sub>-d2 or cAMP-d2 conjugate, respectively (for more information on the principle, see <http://www.htrf.com/products/gpcr/ipone> and <http://www.htrf.com/products/gpcr/camp>).

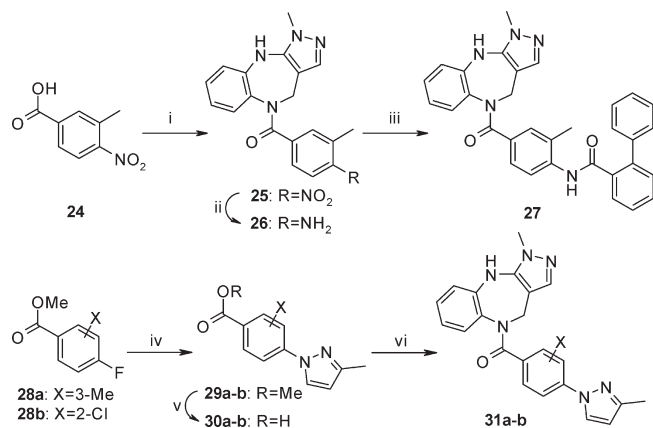
**Molecular Modeling**

A three-dimensional model [model coordinates are available upon request] of the oxytocin receptor was built and refined based on the sequence alignment and the V<sub>1a</sub> model previously published by our group.<sup>37</sup> The quality of this new

model was assessed by docking first the endogenous peptide ligand oxytocin (see Figure S1 in Supporting Information). OT and compound **1** were docked to this preliminary model using the Gold 3.0 program.<sup>38</sup> The starting conformation of OT was modeled from the X-ray structure of neurophysin-bound OT.<sup>39</sup> Compound **1** was built starting from the X-ray structure of its truncated analogue **12c**, and its geometry was fully optimized with HF/6-31\* level using Gaussian 03.<sup>40</sup> The resulting binding mode of compound **1** obtained was similar to the oxytocin binding mode (Figure 3).

**Results and Discussion**

**Full Characterization of Compound 1.** Molecule **1** is the most active of very few nonpeptide oxytocin agonists published to date.<sup>22–24</sup> It results from the optimization of a hit discovered after high throughput screening. The activity of **1** on OT receptor (EC<sub>50</sub> = 33 nM) was characterized using a NFAT-luciferase gene reporter assay. Its agonist activity for

**Scheme 3.** Synthesis of the Molecular Hybrids Conserving the Western Part of Compound **1**<sup>a</sup>


<sup>a</sup> Reagents and conditions: (i) (a) (COCl)<sub>2</sub>, cat. DMF, DCM, 30 min; (b) **7**, Et<sub>3</sub>N, DCM, overnight, 90%. (ii) SnCl<sub>2</sub>·2H<sub>2</sub>O, EtOH, reflux, 1 h, 82%. (iii) (a) 2-Phenylbenzoic acid, (COCl)<sub>2</sub>, cat. DMF, DCM, 5 h; (b) **26**, Et<sub>3</sub>N, DCM, 36 h, 87%. (iv) 3-Methylpyrazole, K<sub>2</sub>CO<sub>3</sub>, NMP, 120 °C, 6–25 h, 9–41%. (v) HCl/H<sub>2</sub>O/AcOH, reflux, 6 h, 96–99%. (vi) (a) SOCl<sub>2</sub>, cat. NMP, DCM, overnight; (b) **7**, pyridine, cat. DMAP, DCM, 3 d, or μw 80 °C, 8 min, 53–81%.

the V<sub>2</sub> receptor subtype (EC<sub>50</sub> = 850 nM) was evaluated in a similar way (CRE-luciferase). Furthermore, **1** was shown to be active in vivo after iv bolus administration in a rat model of uterine response. We have extended the characterization in studying the binding profile of this lead compound at the OT, V<sub>1a</sub>, and V<sub>2</sub> oxytocin and vasopressin receptor subtypes. Furthermore, its agonist and antagonist functional efficacy was directly measured at the level of the second messengers.

In terms of binding affinity, **1** was less potent than expected at the OT receptor with K<sub>i</sub> = 147 nM (Table 1). Its affinity for the V<sub>1a</sub> and V<sub>2</sub> receptor subtypes was K<sub>i</sub> = 330 nM and K<sub>i</sub> > 1000 nM, respectively. In terms of functional efficacy, **1** showed a weak but substantial agonist activity at the OT (K<sub>act</sub> = 667 nM) and V<sub>2</sub> (K<sub>act</sub> = 599 nM) receptors but not at the V<sub>1a</sub> receptor. However, the activation did not reach the level induced by OT or AVP, indicating a partial agonist profile with an E<sub>max</sub> of 58% and 84% for OT and V<sub>2</sub> receptors, respectively. The capacity of **1** to antagonize the endogenous ligand activation was also measured. In the conditions of the study, compound **1** showed some weak antagonist effect at the OT receptor, no significant effect at the V<sub>2</sub> receptor, and a marked V<sub>1a</sub> antagonist effect (K<sub>inact</sub> = 271 nM). Overall, compound **1** is a moderately active ligand of the OT receptor with a marginal selectivity versus the V<sub>1a</sub> receptor and a larger selectivity versus the V<sub>2</sub> site (> 7 fold). At the level of second messengers, it behaves as a partial agonist of the OT and V<sub>2</sub> receptors and as a slightly more potent antagonist at the V<sub>1a</sub> receptor. The apparent discrepancy between the reported EC<sub>50</sub> and full efficacy at OT receptors derived from a gene reporter assay<sup>24</sup> and the affinity and efficacy measured here from radioligand binding and second messenger analysis can easily be explained by the fact that the gene reporter assays reflect a downstream effect with several levels of signal amplification. The extension of profiling to the V<sub>1a</sub> receptor subtype unmasked the weak selectivity of compound **1**, hampering its usefulness as a pharmacological investigation probe. However, this molecule remains a very interesting tool to investigate the ligand–receptor interactions at the molecular level and more particularly the structural

**Table 2.** Structures and Biological Activities of Truncated Analogues of Compound **1**

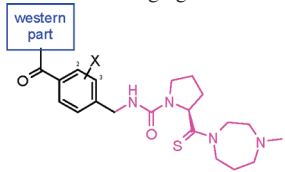
cpd	structure	OT-R			V <sub>1a</sub> -R			V <sub>2</sub> -R		
		K <sub>i</sub> <sup>a</sup>	K <sub>act</sub> <sup>b</sup>	K <sub>inact</sub> <sup>c</sup>	K <sub>i</sub> <sup>a</sup>	K <sub>act</sub> <sup>b</sup>	K <sub>inact</sub> <sup>c</sup>	K <sub>i</sub> <sup>a</sup>	K <sub>act</sub> <sup>b</sup>	K <sub>inact</sub> <sup>c</sup>
<b>1</b>		147 ± 11	667 ± 68 58±2%	16±6%	330 ± 38	ns	271 ± 61	>1000	599 ± 91 84±4%	ns
<b>12a</b>		>1000	ns <sup>d</sup>	37±10%	167 ± 7	ns	187 ± 36	>1000	20±2%	ns
<b>12b</b>		>5000	ns <sup>d</sup>	30±8%	170 ± 12	ns	134 ± 9	>1000	16±2%	ns
<b>12c</b>		>5000	ns <sup>d</sup>	ns	>5000	ns	27±3%	ns	ns	ns

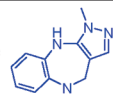
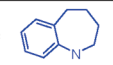
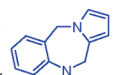
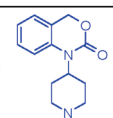
<sup>a</sup> The inhibition constants (K<sub>i</sub> in nM) for human V<sub>1a</sub>, V<sub>2</sub>, and OT receptors were determined on CHO cell membranes by competition binding assays (displacement of radioactive [<sup>3</sup>H]AVP). Results are expressed as mean ± SEM of at least three separate experiments performed in triplicate. When K<sub>i</sub> > 1000 nM, these are results of at least two separate experiments performed in triplicate. <sup>b</sup> The activation constants (K<sub>act</sub> in nM) were measured in CHO cell lines expressing either vasopressin V<sub>1a</sub> or V<sub>2</sub> or oxytocin receptor by IP-One (V<sub>1a</sub>-R and OT-R, IP<sub>1</sub> accumulation) or cAMP dynamic 2 (V<sub>2</sub>-R, cAMP accumulation) assays. These values are the mean ± SEM of at least three separate experiments performed in triplicate. The maximal stimulations (E<sub>max</sub>) are expressed as percentages of the endogenous agonist maximal stimulation (n = 3). In case of a weak stimulation, results are expressed as percentages of the endogenous agonist maximal stimulation at [ligand] = 1 μM (n = 2). Results are not significant (ns) when there is < 10% response at [ligand] = 1 μM (n = 2). <sup>c</sup> The inactivation constants (K<sub>inact</sub> in nM) were measured in CHO cell lines expressing either vasopressin V<sub>1a</sub> or V<sub>2</sub> or oxytocin receptor by IP-One (V<sub>1a</sub>-R and OT-R, inhibition of agonist-induced IP<sub>1</sub> accumulation) or cAMP dynamic 2 (V<sub>2</sub>-R, inhibition of agonist-induced cAMP accumulation) assays. These values are the mean ± SEM of at least three separate experiments performed in triplicate. In case of a weak inhibition, results are expressed as percentages of endogenous agonist-response inhibition at [ligand] = 1 μM (n = 2). Results are not significant (ns) when there is < 10% response inhibition at [ligand] = 1 μM (n = 2). <sup>d</sup> [ligand] up to 10 μM.

determinants of affinity and efficacy in the vasopressin–oxytocin system.

**Determinants for the Agonism/Antagonism Switch.** The binding and the switch from agonist to antagonist among G protein-coupled receptor (GPCR) ligands remain a key issue for drug design. The vasopressin–oxytocin receptors represent a very interesting system to investigate this question. Indeed, the different receptor subtypes are very similar (37% to 47% identity), they are activated by the same endogenous agonist, arginine vasopressin (AVP), they have been cloned in many species including humans,<sup>41</sup> many peptidic and nonpeptidic ligands are known, and three-dimensional models validated by many experimental data are available.<sup>34–37,42–59</sup>

Among the structurally diverse nonpeptide ligands of vasopressin receptors disclosed over the years, the tetrahydrobenzazepine/benzodiazepine series is one of the most important so far. Ligands of this class are active at three of the four receptor subtypes, often exhibiting potent antagonist properties at the V<sub>1a</sub> and/or V<sub>2</sub> receptors, and sometimes a non-negligible OT-R antagonist activity (e.g., compound **2**).<sup>21</sup> To date, very few nonpeptide agonists acting at these receptors have been reported.<sup>22</sup> Interestingly, the only ones

**Table 3.** Structures and Biological Activities of Hybrid Molecules Exchanging the Western Part of **1**


cpd	X	western part	OT-R			V <sub>1a</sub> -R			V <sub>2</sub> -R		
			K <sub>i</sub> <sup>a</sup>	K <sub>act</sub> <sup>b</sup>	K <sub>inact</sub> <sup>c</sup>	K <sub>i</sub> <sup>a</sup>	K <sub>act</sub> <sup>b</sup>	K <sub>inact</sub> <sup>c</sup>	K <sub>i</sub> <sup>a</sup>	K <sub>act</sub> <sup>b</sup>	K <sub>inact</sub> <sup>c</sup>
<b>1</b>	3-Me		147 ± 11	667 ± 68 58±2%	16±6%	330 ± 38	ns	271 ± 61	>1000	599 ± 91 84±4%	ns
<b>23a</b>	3-Me		844 ± 100	2700 ± 170 53±6%	ns	633 ± 101	ns	33±2%	>1000	245 ± 46 86±2%	ns
<b>23b</b>	3-Me		2500 ± 270 <sup>d</sup>	110000 ± 14000 50.6±0.6% <sup>e</sup>	ns <sup>f</sup>	>1000	ns	754 ± 146	3400 ± 60 <sup>d</sup>	9±4% <sup>e</sup>	17±8% <sup>f</sup>
<b>23c</b>	2-Cl		>5000	ns <sup>g</sup>	ns <sup>h</sup>	>5000	ns <sup>g</sup>	ns <sup>h</sup>	>5000	ns <sup>g</sup>	ns <sup>h</sup>
<b>23d</b>	3-Me		245 ± 15	ns <sup>i</sup>	383 ± 40	>5000	ns	ns	ns	ns	ns

<sup>a</sup> The inhibition constants ( $K_i$  in nM) for human V<sub>1a</sub>, V<sub>2</sub>, and OT receptors were determined on CHO cell membranes by competition binding assays (displacement of radioactive [<sup>3</sup>H]AVP). Results are expressed as mean ± SEM of at least three separate experiments performed in triplicate. When  $K_i > 1000$  nM, these are results of at least two separate experiments performed in triplicate. <sup>b</sup> The activation constants ( $K_{act}$  in nM) were measured in CHO cell lines expressing either vasopressin V<sub>1a</sub> or V<sub>2</sub> or oxytocin receptor by IP-One (V<sub>1a</sub>-R and OT-R, IP<sub>1</sub> accumulation) or cAMP dynamic 2 (V<sub>2</sub>-R, cAMP accumulation) assays. These values are the mean ± SEM of at least three separate experiments performed in triplicate. The maximal stimulations ( $E_{max}$ ) are expressed as percentages of the endogenous agonist maximal stimulation ( $n = 3$ ). In case of a weak stimulation, results are expressed as percentages of the endogenous agonist maximal stimulation at [ligand] = 1  $\mu$ M ( $n = 2$ ). Results are not significant (ns) when there is < 10% response at [ligand] = 1  $\mu$ M ( $n = 2$ ). <sup>c</sup> The inactivation constants ( $K_{inact}$  in nM) were measured in CHO cell lines expressing either vasopressin V<sub>1a</sub> or V<sub>2</sub> or oxytocin receptor by IP-One (V<sub>1a</sub>-R and OT-R, inhibition of agonist-induced IP<sub>1</sub> accumulation) or cAMP dynamic 2 (V<sub>2</sub>-R, inhibition of agonist-induced cAMP accumulation) assays. These values are the mean ± SEM of at least three separate experiments performed in triplicate. In case of a weak inhibition, results are expressed as percentages of endogenous agonist-response inhibition at [ligand] = 1  $\mu$ M ( $n = 2$ ). Results are not significant (ns) when there is < 10% response inhibition at [ligand] = 1  $\mu$ M ( $n = 2$ ). <sup>d</sup>  $n = 2$ . <sup>e</sup> V<sub>2</sub>-R: 13 ± 1% of response at 10  $\mu$ M ( $n = 3$ ); OT-R: maximal stimulation could not be reached at 100  $\mu$ M. <sup>f</sup> V<sub>2</sub>-R: 43 ± 6% of inhibition at 10  $\mu$ M ( $n = 3$ ); OT-R: 11 ± 16% ( $n = 2$ ) and 56% ( $n = 1$ ) at 10 and 100  $\mu$ M, respectively. <sup>g</sup> [ligand] up to 100  $\mu$ M ( $n = 3$ ). <sup>h</sup> Inhibition at 10 and 100  $\mu$ M, respectively ( $n = 2$ ): V<sub>1a</sub>-R: 7.0 ± 0.8% and 92 ± 2%, V<sub>2</sub>-R: 25 ± 1% and 94 ± 1%, OT-R: 17 ± 12% and 52 ± 14%. <sup>i</sup> [ligand] up to 10  $\mu$ M ( $n = 3$ ).

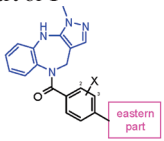
belong to the benzazepine series (e.g., compound **3**).<sup>27,60–62</sup> Their V<sub>2</sub>-R agonist properties were discovered as a result of structural modifications of the antagonists.<sup>33,63</sup> Intriguingly, the first nonpeptide OT-R agonist (compound **1**) is also related to the said chemical class.<sup>24</sup> Therefore, a systematic study of these remarkably subtle relationships between these particular ligands should be of outstanding interest to clarify the structural determinants conferring them such agonist/antagonist properties.

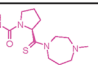
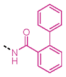
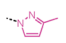

Thus, in our attempts to understand the structural origin of compound **1** OT receptor agonist activity, we decided to cleave the structure progressively or to combine its fragments with fragments from a reported nonselective V<sub>1a</sub>/V<sub>2</sub>/OT receptor antagonist, compound **2**, a V<sub>2</sub> receptor agonist, WAY-VNA-932, compound **3**, and a benzoxazinone-type selective OT receptor antagonist, L-371,257, compound **4**. The affinity and efficacy on second messenger activation of the resulting products have been determined.

**Truncated Analogues.** As seen from Table 2, the removal of the thioamide-homopiperazine from compound **1** (compound **12a**) led to a very significant decrease in affinity for OT-R because a very low [<sup>3</sup>H]AVP displacement could be observed at a 1  $\mu$ M concentration. No agonist activity could be detected, and a 37% inhibition of the response induced by OT could be observed at 1  $\mu$ M, suggesting a weak and

marginally reinforced antagonist effect compared to **1**. Additional cleavage leading to the urea **12b** and to the acetamide **12c** resulted in a complete loss of affinity and efficacy for the OT receptor. Again, some weak but significant antagonistic activity could still be detected for **12b**. One may then conclude that the eastern fragment of molecule **1** contributes significantly to its affinity for the OT receptor. The lack of agonist efficacy and some residual antagonist activity in compound **12a** suggested that the homopiperazine fragment is necessary for the OT receptor activation. The same trend was observed on the V<sub>2</sub> receptor subtype. The initial affinity was very weak and remained as such in compounds **12a** and **12b**. However, in contrast to OT-R, the agonist character persisted in the series of analogues although very weakened. No antagonist activity could be detected. Finally, on the V<sub>1a</sub> receptor subtype, the affinity was slightly reinforced upon truncating the molecule, as indicated by both the affinity and the antagonist efficacy of **1**, **12a**, and **12b**. However, the ultimate transformation of the urea in **12b** into an acetamide in **12c** was completely detrimental to the activity.

This first part of the study highlighted the crucial role of the entire chain for the OT-R affinity of **1** and the specific contribution of the homopiperazine fragment to its agonist efficacy. Unexpectedly, it also highlighted the divergent

**Table 4.** Structures and Biological Activities of Hybrid Molecules Exchanging the Eastern part of **1**


cpd	X	eastern part	OT-R			V <sub>1a</sub> -R			V <sub>2</sub> -R		
			K <sub>i</sub> <sup>a</sup>	K <sub>act</sub> <sup>b</sup>	K <sub>inact</sub> <sup>c</sup>	K <sub>i</sub> <sup>a</sup>	K <sub>act</sub> <sup>b</sup>	K <sub>inact</sub> <sup>c</sup>	K <sub>i</sub> <sup>a</sup>	K <sub>act</sub> <sup>b</sup>	K <sub>inact</sub> <sup>c</sup>
<b>1</b>	3-Me		147 ± 11	667 ± 68 58 ± 2%	16 ± 6%	330 ± 38	ns	271 ± 61	>1000	599 ± 91 84 ± 4%	ns
<b>27</b>	3-Me		111 ± 5	ns <sup>d</sup>	557 ± 32	37 ± 6	ns	412 ± 55	6.4 ± 1.0	ns	1.10 ± 0.30
<b>31a</b>	3-Me		27.8 ± 0.6	ns <sup>d</sup>	14.8 ± 1.5	18 ± 3	ns	32 ± 5	913 ± 55	ns	253 ± 69
<b>31b</b>	2-Cl		17 ± 3	ns	69 ± 45	27 ± 4	ns	13 ± 3	29 ± 5	8.4 ± 0.4 94 ± 6%	ns

<sup>a</sup>The inhibition constants ( $K_i$  in nM) for human V<sub>1a</sub>, V<sub>2</sub>, and OT receptors were determined on CHO cell membranes by competition binding assays (displacement of radioactive [<sup>3</sup>H]AVP). Results are expressed as mean ± SEM of at least three separate experiments performed in triplicate. When  $K_i > 1000$  nM, these are results of at least two separate experiments performed in triplicate. <sup>b</sup>The activation constants ( $K_{act}$  in nM) were measured in CHO cell lines expressing either vasopressin V<sub>1a</sub> or V<sub>2</sub> or oxytocin receptor by IP-One (V<sub>1a</sub>-R and OT-R, IP<sub>1</sub> accumulation) or cAMP dynamic 2 (V<sub>2</sub>-R, cAMP accumulation) assays. These values are the mean ± SEM of at least three separate experiments performed in triplicate. The maximal stimulations ( $E_{max}$ ) are expressed as percentages of the endogenous agonist maximal stimulation ( $n = 3$ ). In case of a weak stimulation, results are expressed as percentages of the endogenous agonist maximal stimulation at [ligand] = 1 μM ( $n = 2$ ). Results are not significant (ns) when there is < 10% response at [ligand] = 1 μM ( $n = 2$ ). <sup>c</sup>The inactivation constants ( $K_{inact}$  in nM) were measured in CHO cell lines expressing either vasopressin V<sub>1a</sub> or V<sub>2</sub> or oxytocin receptor by IP-One (V<sub>1a</sub>-R and OT-R, inhibition of agonist-induced IP<sub>1</sub> accumulation) or cAMP dynamic 2 (V<sub>2</sub>-R, inhibition of agonist-induced cAMP accumulation) assays. These values are the mean ± SEM of at least three separate experiments performed in triplicate. In case of a weak inhibition, results are expressed as percentages of endogenous agonist-response inhibition at [ligand] = 1 μM ( $n = 2$ ). Results are not significant (ns) when there is < 10% response inhibition at [ligand] = 1 μM ( $n = 2$ ). <sup>d</sup>[ligand] up to 10 μM ( $n = 3$ ).

structure–activity relationships among highly similar receptor subtypes because structural variations led to a loss of affinity and a switch from agonism to antagonism in one case (OT-R), a retention of affinity and agonist efficacy in a second case (V<sub>2</sub>-R) and an increase in affinity and antagonist efficacy in the last case (V<sub>1a</sub>-R) (Figure 1).

**Hybrid Molecules.** To further explore this SAR divergence, we prepared and analyzed the hybrid molecules in Tables 3 and 4. A simple qualitative analysis of these ligands strongly suggested a shared pharmacophore around a central benzoyl fragment branched with a polycyclic aromatic amide on the western side and an aromatic or electron-rich side chain on the opposite para position (eastern). It was tempting to assume that similar fragments bind to similar regions and trigger similar effects in the highly homologous receptor subtypes.

The contribution of the western tricyclic part was first studied. Unexpectedly, despite the fact that compounds **2**, **3**, and **4** had a good or very good affinity for the OT-R, better or comparable to **1**, the introduction of their aromatic fragments in the structure of **1** led to a significant (**23a,b,d**) to dramatic (**23c**) decrease in affinity for the OT receptor (Table 3). The efficacy decreased in a parallel fashion for **23a**

and **23b**. Even more surprisingly, the chimeric ligand **23d** switched from OT agonist to OT antagonist upon this ring replacement. In a general manner, the affinity and efficacy on the V<sub>1a</sub> and V<sub>2</sub> homologous receptors were also decreased without change in the efficacy profile.

These results led to two conclusions. The highly similar cyclic aromatic fragments of the different ligands do not contribute in the same way to their activity, probably interacting in different manners with a given receptor as well as with the different homologous receptor subtypes. The aromatic cyclic fragments of molecules **1**, **2**, and **3** stabilize the active conformation of the OT receptor, whereas the piperidino-benzoxazinone of **4** stabilizes an inactive conformation. Interestingly, both benzazepine and piperidino-benzoxazinone moieties actually derive from structural modifications of the quinolinone ligand OPC-21268, the first nonpeptide vasopressin receptor ligand described.<sup>28,64,65</sup> Structurally speaking, there is a reasonably good similarity between the piperidino-benzoxazinone fragment of **4** and the benzazepine moiety. They both contain a cyclic aromatic moiety likely to interact with aromatic residues in the active site. They are both connected to the rest of the molecules by an amide link. The discriminant feature could be the distance between the aromatic ring and the amide link that is slightly superior in the piperidino-benzoxazinone moiety.

The contribution of the eastern part of the molecule was then investigated by introducing the side chains of compounds **2** and **3** on the central and western part of **1**. Once again, the results were quite unexpected (Table 4). The replacement of the complex electronegative side chain in **1** by the hydrophobic biphenyl amide of **2** led to compound **27** with a conserved OT receptor affinity ( $K_i = 111$  nM versus 147 nM). The replacement by the methyl pyrazole directly branched on the central benzoyl core provided **31a**, an even more potent OT-R ligand with a  $K_i = 27.8$  nM. This significant increase was unexpected because compounds **2** and **3** have affinity constants similar to **1** ( $K_i = 109$  and 199 nM, respectively). However, these replacements caused a switch in functional efficacy because compounds **27** and **31a** are potent OT receptor antagonists ( $K_{inact} = 557$  and 14.8 nM, respectively) without any detectable agonist activity. These results highlight the critical contribution of the large electron-rich side chain of **1** to its OT receptor activating properties. Replacement by smaller, more hydrophobic fragments increases the affinity but locks the receptor in an inactive conformation. A similar effect was observed on the V<sub>2</sub> receptor subtype. Compound **27** is also a potent and selective V<sub>2</sub> receptor antagonist ( $K_i = 6.4$  nM, V<sub>2</sub>/V<sub>1a</sub>  $K_{inact}$  ratio = 374, V<sub>2</sub>/OT  $K_{inact}$  ratio = 506). In addition, the affinity for the V<sub>1a</sub> receptor subtype increased from 10- to 20-fold (compounds **27** and **31a**, respectively) but the initial antagonist activity was retained.

Of interest is also the differential action of the core benzoyl nucleus common to all ligands. With a methyl group in position 3, the compound **31a** is a potent antagonist for the V<sub>1a</sub> and OT receptors and a weak antagonist for the V<sub>2</sub> receptor. Substitution of the methyl for a chlorine in position 2 led to an equipotent ligand (**31b**) for the three receptor subtypes. However, **31b** behaves as a full agonist at the V<sub>2</sub> and as an antagonist at the V<sub>1a</sub> and OT receptor subtypes, highlighting once more the divergent SAR among highly homologous ligands acting at highly homologous receptors. Furthermore, by applying the same modification when having the large side chain of **1**, the affinity for the three

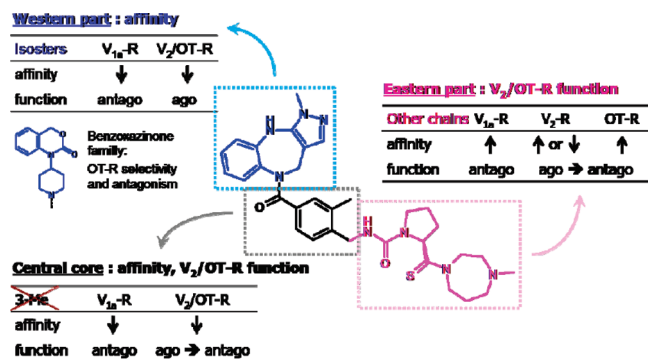


**Figure 2.** Schematic representation of the main results of the hybrid molecules of compound **1**.

receptor subtypes is dramatically lost, as illustrated by compounds **23b** and **23c** (Table 3). Therefore, one may hypothesize that a methyl group on the central benzoyl core seems to be required at position 3 to stabilize this flexible chain in its active conformation.

The second part of this study highlighted the contribution to affinity, efficacy, and specificity of each fragment of the compound **1**. With regard to the western tricyclic part, the benzazepine polycyclic moiety contributes to the affinity and the stabilization of the active conformation of the OT and V<sub>2</sub> receptors, the pyrazolobenzodiazepine scaffold of **1** remaining unequaled (Figure 2). By contrast, the piperidino-benzoxazinone is responsible for the OT-R selectivity and stabilizes an inactive conformation of this receptor. Clearly, both scaffolds are not interchangeable. Regarding the eastern part of the molecule, the large electron-rich side chain of **1** is essential for the oxytocin receptor activation. Finally, the core benzoyl nucleus is not just a common linker but can lock/unlock a specific conformation of the ligand through its different substitution patterns.

In summary, the design and synthesis of several truncated analogues of **1** and of hybrid molecules enabled us to identify the key structural features responsible for its affinity and OT-R agonist efficacy. Although it was tempting to assume that similar fragments bind to similar regions and trigger similar effects in the highly homologous receptor subtypes, the reality is definitely not so straightforward. Indeed, each part of the molecule appears to play a specific role for its activity on the oxytocin receptor, and quite surprising findings arose from this systematic study regarding its behavior toward the other vasopressin receptor subtypes. The main conclusion remains that the OT-R agonist activity of compound **1** is mainly conferred by this large, rather polar, pseudopeptidic side chain present at its eastern part. The cleavage of this polar side chain and its replacement by a smaller group did not afford an OT-R agonist as it does with the same backbone on the V<sub>2</sub>-R.<sup>33,63</sup> For bioamine receptors ligands, which have to reach a deep binding cleft between the helices, agonists are typically smaller than antagonists.<sup>66,67</sup> Indeed, the switch from an antagonist to an agonist for nonpeptide receptors is generally achieved by the suppression of a bulky lipophilic side chain. Obviously, it may be more subtle for peptide receptor ligands, whose binding site also includes the extracellular region. The large size of peptides often allows the discrimination of the binding and the activation domains, both on the peptide ligand and the target receptor. This address and message concept has been widely explored and often validated.<sup>46,49,54,68,69</sup> A priori, this

separation renders the design of small size, potent agonists more difficult. However, morphine represents a very good example showing that a small nonpeptide molecule is able to mimic a peptide in combining affinity and functional activity on a limited molecular entity. Furthermore, the switch from agonist to antagonist on morphine skeleton follows essentially the same rules as for biogenic amine receptor ligands and can be achieved by substitution with hydrophobic fragments.<sup>70</sup> By contrast, other examples have shown that a nonpeptide antagonist ligand of a peptide receptor could be converted into an agonist by introduction of an additional hydrophobic interaction or steric constraint.<sup>69,71,72</sup> This phenomenon has also been studied on several receptors via mutagenesis and photoaffinity labeling of structurally similar agonist and antagonist ligands.<sup>73–87</sup> As shown here, the side-chain decrease strategy leads indeed to a conserved agonist character or a switch from antagonist to agonist for the V<sub>2</sub> receptor subtype but did not operate for the OT and V<sub>1a</sub> receptors, demonstrating that the structural determinants of the antagonist/agonist switch are probably specific to every receptor–ligand complex. We have attempted to obtain an explanation for these observed subtle affinity and efficacy switches in analyzing molecular models of the OT receptor binding to OT, the endogenous ligand, or to compound **1**, a partial agonist.

**Molecular Modeling.** Models for the OT, V<sub>1a</sub>, V<sub>1b</sub>, and V<sub>2</sub> receptors interacting with diverse ligands had previously been proposed and partly validated experimentally.<sup>42–59</sup> They were derived from reference GPCR experimental structures with different levels of relevance and resolution. However, they proved to be sufficiently qualitative to predict binding pocket localization, residues responsible for affinity, species, and receptor specificity. We attempted to go one step further in understanding the agonism–antagonism switch for compound **1** using the best current reference templates for GPCR modeling. A three-dimensional model of the oxytocin receptor was built and refined based on the sequence alignment and the V<sub>1a</sub> model previously published by our group.<sup>37</sup> The quality of this new model was assessed by docking the endogenous peptide ligand oxytocin (see Figure S1 in Supporting Information). In agreement with most studies, the hydrophobic part of oxytocin (Tyr2 and Ile3) is accommodated by a hydrophobic pocket (M3.36, W6.48, F6.51) lying in the deep 7-transmembrane (TM) cavity between TMs III, V, VI, and VII. An important H-bonds network is established between the conserved glutamine residues (Q3.32, Q4.60, Q6.55) located at the upper rim of the cavity and the polar part of the peptide hormone, i.e., the main chain atoms as well as Gln4, Asn5, and also the Tyr2 side chain. Similar interactions have also been described for AVP into V<sub>1a</sub>-R and V<sub>1b</sub>-R in our most recent models<sup>37</sup> as well as in previously published binding modes.<sup>43,48</sup> Moreover, the N-terminal Gly9 of OT is interacting with E1.35 via hydrogen bonding. Thus, a very tiny network of hydrogen bonds is used to anchor OT to its receptor. On the other hand, Leu8 of OT is pointed to the F2.68, located close to the extracellular loop E1, as proposed previously.<sup>44</sup> Noteworthy, most residues proposed to participate in OT binding have been shown to be of crucial importance for AVP agonist peptide binding using site-directed mutagenesis.<sup>43,48,49</sup> Thus, although our OT binding has not been experimentally validated, we believe that our OT-R model is a good starting point for docking other agonists.

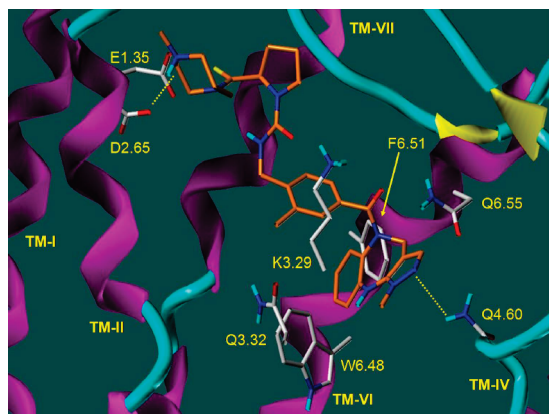


**Figure 3.** Proposed binding mode of compound **1** to human OT receptor. The seven TM helices of each receptor are displayed by cylinders and labeled from I to VII. Some TM helices have been omitted for clarity. Compound **1** is displayed by orange sticks. This figure and Figure S1 in Supporting Information has been prepared with Sybyl.<sup>99</sup>

Compound **1** was docked in this model in an attempt to gain insight into the agonism–antagonism switch. The resulting binding mode obtained was similar to the oxytocin binding mode (Figure 3). More precisely, a well-defined negatively charged subsite (E1.35, D2.65) perfectly accommodates the positively charged basic amine at the eastern part of compound **1**. Very recently, we demonstrated that this subsite represents a key anchoring point for the Arg8 residue of AVP and related peptide agonists in  $V_{1a}$  and  $V_{1b}$  receptors.<sup>37</sup> The western part of compound **1** is anchored via H-bonds formed between its nitrogen-enriched tricyclic fused ring and the conserved Q4.60 as well as the carbonyl belonging to the backbone of K3.29. A possible aromatic stacking interaction is also likely between the central benzene ring of the ligand and the conserved F6.51 of the receptor.

Consequently, this novel oxytocin nonpeptide agonist series represented by compound **1** seems to bind to the receptor in a similar way that the peptide ligand does. The extended pseudopeptidic structure of **1** seems to mimic the size and the shape of oxytocin itself and to establish the interactions necessary to activate the oxytocin receptor. Indeed, our results indicate that the end of the eastern part of compound **1** is required for OT-R activation and one can imagine that the basic amine of the homopiperazine fragment would be the key anchoring point to the receptor in order to confer agonism to the ligand. According to our model, this nitrogen can be in close contact with three possible acidic residues of the OT receptor, namely E1.35, D2.65 and the conserved D of the extracellular loop E2. Interestingly, only D2.65 is not conserved in the  $V_2$  receptor, where it is replaced by a K. This might explain why compound **1** has a very low affinity and efficacy for the  $V_2$  receptor which binds and responds to the small hydrophobic agonist WAY-VNA-932. Nevertheless, this model is not sufficient to explain the agonism of compound **1** at the OT receptor and its antagonism at the  $V_{1a}$  receptor because oxytocin itself has no positive charge at the region considered and the three acidic residues are conserved in  $V_{1a}$ -R.

Thus, studying the GPCR activation mechanisms still remains challenging. A lot of work has been done on the rhodopsin and the  $\beta_2$ -adrenergic class 1 receptors.<sup>88,89</sup> According to the proposed toggle switch model,<sup>89</sup> a 90° rotation of the crucial conserved W6.48 side chain would

lead to the movement of TM VI and TM VII around the highly conserved proline kinks, while the intracellular segments would move away from TM III to expose specific epitopes, and the extracellular segments would get closer to TM III to close the binding site. The receptor would be maintained in its inactive conformation by an aromatic cluster in TM V and VI, stabilizing the W6.48. The antagonist binding mode is located deep in the transmembrane domain and based on sufficiently strong interactions with the hydrophobic and aromatic residues of TM IV, V, VI, and VII, in order to prevent W6.48 rotation, maintaining the receptor in its inactive conformation. The agonist would adopt a more superficial binding mode between TM III, VI, and VII and close to TM III to allow rotation of the W6.48 located at the opposite part of the cavity. Established interactions are thus rather polar, with some hydrophobic contacts able to disturb the aromatic cluster. In stabilizing the active receptor conformation, small agonists would act as a molecular *glue* in the main cavity between the helices, whereas peptides would play the role of Velcro at the upper helical bundle and the extracellular loops, to maintain these helices together for an extended time. Small  $V_2$ -R agonists would bind in a position close to TM III to not disturb the W6.48 rotation. Because of subtle differences of topology of the cavity in OT-R, interaction of these ligands with the aromatic cluster of TM VI would be too strong. On the contrary, the eastern chain of the OT-R agonist **1** would bring additional interactions with the upper part of TM I and II, allowing the molecule to move upward, thus acting as Velcro in peptide mimicry.

## Conclusions

The binding mode and the switch from antagonist to agonist among GPCR ligands remain a key issue for drug design. The vasopressin–oxytocin receptors and their ligands represent a very convenient model system to address such an issue because highly homologous ligands binding to highly homologous binding sites are known. We have explored the affinity and efficacy shifts around compound **1**, which is the lead of the first series of oxytocin receptor nonpeptide agonists described to date. We have fully investigated its binding and efficacy profiles on the OT,  $V_{1a}$ , and  $V_2$  oxytocin–vasopressin receptors. The first important result is that compound **1** is not a specific, full OT-R agonist. In our hands, it displays only a 2-fold selectivity versus the  $V_{1a}$  receptor in terms of binding and behaves as a *partial* agonist (58%) at the OT-R, being equipotent as a  $V_2$ -R agonist and more potent as a  $V_{1a}$ -R antagonist. This, added to its poor bioavailability, preempts its use as specific pharmacological probe for studying oxytocin-related functional responses. It remains, however, a very interesting and relevant tool to explore the oxytocin binding and efficacy supramolecular determinants. Its study leads to the second conclusion that structure–activity relationships around vasopressin/oxytocin ligands are extremely subtle and the determinants for the antagonism/agonism switch are very difficult to identify. Thus, although qualitatively accurate, three-dimensional models of GPCR still remain of weak predictive value to address such subtle phenomenon that might be under kinetic and/or polymolecular control. Indeed, static models can not satisfactory take into account dynamic processes, conformational changes, loops movements, solvation/desolvation, allosteric interactions, dimerization/oligomerization,<sup>90</sup> G protein binding, membrane environment, and



the multitude of parameters intervening in a living cell. Molecular modeling of GPCR, associated with extended experimental validation, is definitely an additive value to drug design but, in our hands and in this particular case study, it reaches its limits. The recent crystallographic structure of the adenosine A<sub>2A</sub> receptor further highlights the plasticity of GPCRs and the difficulty to predict precisely a given ligand binding mode.<sup>91</sup> Thus, for the time being, the dual challenge of discovering a full, bioavailable OT agonist on one hand and rationally designing a nonpeptide agonist for a peptide receptor on the other hand remains open. However, waiting for an oxytocin receptor crystallographic structure and having in mind that peptide GPCRs represent targets of special interest for novel therapeutics,<sup>92,93</sup> we will continue to combine molecular modeling, SAR studies, labeling,<sup>34–36,55</sup> and mutagenesis to take up the challenge.

## Experimental Section

**Chemistry: General Methods.** Dry solvents were purchased from Fluka (SureSeal). Microwaves irradiations were performed on a Biotage Initiator 2.0 apparatus. Melting points (mp) were determined with a Gallenkamp apparatus and are uncorrected. Optical rotations ( $[\alpha]_D$ ) were determined with a Perkin-Elmer 241 MC or a Perkin-Elmer 341 polarimeter. <sup>1</sup>H and <sup>13</sup>C NMR spectra were recorded at 298 K on Bruker spectrometers at 200 or 300 and 50 or 75 MHz, respectively, in CDCl<sub>3</sub>, DMSO-*d*<sub>6</sub>, or CD<sub>3</sub>OD, using residual solvent as an internal reference. Chemical shifts ( $\delta$ ) are reported in parts per million (ppm), coupling constants (*J*) are reported in hertz (Hz). IR spectra ( $\nu$ , cm<sup>-1</sup>) were obtained with a Perkin-Elmer FT-IR 1600 or a Perkin-Elmer FT-IR 2000 spectrometers, or with a Thermo Nicolet 380 spectrometer using attenuated total reflection (ATR) technology. Mass spectra (MS) were recorded on a Mariner 5155 from Applied Biosystems using electrospray (ES) ionization mode and a time-of-flight (TOF) analyzer. High resolution mass spectra (HRMS) were recorded on a MicroToF mass spectrometer from Bruker using electrospray (ES) ionization mode and a time-of-flight (TOF) analyzer. Thin-layer chromatography (TLC) was performed on silica gel 60 F<sub>254</sub> aluminum plates from Merck. Flash chromatography was performed on silica gel 60 (230–400 mesh ASTM) from Merck. Analytical RP-HPLC analyses were performed on a Symmetry Shield column (4.6 mm × 150 mm, 5  $\mu$ m, C<sub>18</sub>) from Waters under the following conditions: buffer A, 0.1% aqueous TFA; buffer B, 0.1% TFA in 8:2 CH<sub>3</sub>CN/H<sub>2</sub>O; buffer C, 0.1% TFA in CH<sub>3</sub>CN; gradient 1: 0% buffer B in buffer A for 5 min then 0–100% buffer B in buffer A over 25 min with a flow rate of 0.8 mL/min; gradient 2, 0–100% buffer C in buffer A over 30 min with a flow rate of 1 mL/min; detection:  $\lambda$  = 220/254 nm. Retention times (*t*<sub>R</sub>) from analytical RP-HPLC are reported in minutes. Semipreparative RP-HPLC separations were performed on a Symmetry Shield column (19 mm × 300 mm, 0.7  $\mu$ m, C<sub>18</sub>) from Waters under the following conditions: flow rate: 10 mL/min; buffer A, 0.1% aqueous TFA, buffer B, 0.1% TFA in CH<sub>3</sub>CN; gradients (variable): 0–100% buffer B over 30 min; detection:  $\lambda$  = 220/254 nm. Purity of all target compounds was determined by analytical RP-HPLC according to the conditions described above, and was > 95%.

**1-Methyl-5,10-dihydropyrazolo[3,4-*b*][1,5]benzodiazepin-4(1*H*)-one (6).** A solution of **5** (1.42 g, 5.45 mmol) in a 9:1 *i*PrOH/AcOH mixture (25 mL) was heated in a sealed tube at 160 °C under argon. After 48 h, the resulting mixture was allowed to stand at rt under argon for 1 or 2 days until complete crystallization of the product. The creamy to pale-gray crystals were then collected, washed with cold Et<sub>2</sub>O, and dried under high vacuum to yield the title compound (1.04 g, 89%); mp 262–264 °C. <sup>1</sup>H NMR (300 MHz, DMSO-*d*<sub>6</sub>)  $\delta$  3.66 (s, 3H), 6.75–6.95 (m, 3H), 7.03 (d, 1H, *J* = 7.5 Hz), 7.45 (s, 1H), 8.35 (bs, 1H), 8.96

(bs, 1H). <sup>13</sup>C NMR (75 MHz, DMSO-*d*<sub>6</sub>)  $\delta$  35.0, 100.5, 120.3, 121.8, 123.4, 123.9, 129.4, 133.8, 139.9, 146.0, 163.8. IR (KBr)  $\nu$  (cm<sup>-1</sup>) 3310, 3221, 3098, 3056, 1636, 1615, 1584, 1504, 1446, 1421, 1398, 1329, 1268, 1206, 747.

**1-Methyl-1,4,5,10-tetrahydropyrazolo[3,4-*b*][1,5]benzodiazepine (7).** To a stirred suspension of **6** (714 mg, 3.33 mmol) in dry THF at 0 °C under argon was added portionwise LiAlH<sub>4</sub> (1.01 g, 26.67 mmol) over 10–15 min. The resulting reaction mixture was stirred at 0 °C for 15 min and was then refluxed. After 26 h, as TLC showed incomplete reaction, an additional amount of LiAlH<sub>4</sub> (755 mg, 20.00 mmol) was added. After 44 h refluxing, the reaction mixture was cooled to 0 °C and 35% NaOH (4 mL) was added dropwise over 1 h. Stirring was continued at rt for 1 h, then the mixture was filtered over celite and concentrated in vacuo. Flash chromatography (DCM to 95:5 DCM/MeOH) afforded the title compound as a brown foam (576 mg, 86%); mp 204–206 °C (from MeOH). <sup>1</sup>H NMR (200 MHz, CD<sub>3</sub>OD)  $\delta$  3.71 (s, 3H), 3.98 (s, 2H), 6.65–6.95 (m, 3H), 6.95–7.15 (m, 2H). <sup>13</sup>C NMR (75 MHz, CD<sub>3</sub>OD)  $\delta$  34.9, 45.6, 103.0, 120.5, 122.5, 123.6, 124.1, 135.4, 136.8, 139.9, 143.1. IR (KBr)  $\nu$  (cm<sup>-1</sup>) 3364, 3262, 3153, 3049, 2980, 2791, 1607, 1574, 1506, 1490, 1432, 1395, 1318, 1292, 1247, 993, 821, 757. MS (ES) *m/z* 201.12 ([M + H]<sup>+</sup>).

**2-Methyl-4-[(1-methyl-4,10-dihydropyrazolo[3,4-*b*][1,5]benzodiazepin-5(1*H*)-yl) carbonyl]benzonitrile (9).** To a stirred suspension of **8** (1.10 g, 6.81 mmol) in dry DCM (8 mL) at 0 °C under argon were added successively dry DMF (5 drops) and (COCl)<sub>2</sub> (1.17 mL, 13.61 mmol). The resulting reaction mixture was stirred at 0 °C for 15 min and then was allowed to warm to rt and stirring was continued for 2 h. The solvent was removed in vacuo, and the resulting residue was dissolved in dry THF. The solvent was removed in vacuo, and the resulting residue was dried under high vacuum for 30 min. The resulting brown solid was dissolved in dry DCM (5 mL), and this mixture was added dropwise, under argon, to a stirred ice-cold solution of **7** (1.14 g, 5.69 mmol) and Et<sub>3</sub>N (1.60 mL, 11.38 mmol) in dry DCM (10 mL). Stirring was continued at 0 °C for 30 min and then at rt overnight. As TLC showed still presence of some starting amine **7**, an additional amount of acyl chloride was prepared from the acid **8** (458 mg, 2.28 mmol), dissolved in dry DCM (2 mL) with Et<sub>3</sub>N (0.80 mL, 5.69 mmol), and added dropwise to the ice-cold reaction mixture. Stirring was continued at rt overnight and then the solvent was removed in vacuo. The resulting residue was taken up in DCM (50 mL) and 0.3 M KHSO<sub>4</sub> (75 mL). The aqueous phase was separated and extracted with a 8:2 CHCl<sub>3</sub>/*i*PrOH mixture (100 then 50 mL). The combined organic layers were washed with satd NaHCO<sub>3</sub> (75 mL), dried (Na<sub>2</sub>SO<sub>4</sub>), and concentrated in vacuo to yield a residue that was triturated in AcOEt. The precipitate was filtered, washed with AcOEt, and dried under high vacuum to yield the title compound as a pale-yellow powder (1.46 g, 75%); mp 253–256 °C. <sup>1</sup>H NMR (300 MHz, DMSO-*d*<sub>6</sub>)  $\delta$  2.34 (s, 3H), 3.77 (s, 3H), 3.95 (d, 1H, *J* = 14.3 Hz), 5.64 (d, 1H, *J* = 14.3 Hz), 6.64 (t, 1H, *J* = 7.5 Hz), 6.79 (d, 1H, *J* = 7.9 Hz), 7.01 (d, 1H, *J* = 7.9 Hz), 7.12 (t, 1H, *J* = 7.5 Hz), 7.19 (s, 1H), 7.23–7.33 (m, 2H), 7.55 (d, 1H, *J* = 7.9 Hz), 8.67 (bs, 1H). <sup>13</sup>C NMR (50 MHz, DMSO-*d*<sub>6</sub>)  $\delta$  19.7, 35.4, 43.2, 100.0, 112.2, 117.3, 119.5, 121.2, 124.8, 128.7, 129.0, 130.4, 131.3, 131.9, 135.6, 139.1, 139.6, 140.8, 141.3, 166.9. IR (KBr)  $\nu$  (cm<sup>-1</sup>) 3339, 2910, 2863, 2225, 1633, 1606, 1563, 1504, 1449, 1419, 1387, 1321, 1298, 1251, 1176, 1139, 991, 840, 818, 767.

**1-{2-Methyl-4-[(1-methyl-4,10-dihydropyrazolo[3,4-*b*][1,5]benzodiazepin-5(1*H*)-yl) carbonyl]phenyl}methanamine (10).** To a stirred suspension of **9** (49.6 mg, 0.144 mmol) and CoCl<sub>2</sub>·6H<sub>2</sub>O (70.1 mg, 0.289 mmol) in MeOH (1.5 mL) at 0 °C under argon was added portionwise NaBH<sub>4</sub> (55.7 mg, 1.444 mmol) over 5 min. The resulting black reaction mixture was stirred at 0 °C for 10 min and then was allowed to warm to rt, and stirring was continued for 1 h. After neutralization (pH 7–8) with 1 M KHSO<sub>4</sub> (2 mL), MeOH was removed in vacuo, and the resulting aqueous residue was diluted with 1 M KHSO<sub>4</sub> (15 mL).

This aqueous phase was filtered over celite, extracted with Et<sub>2</sub>O (2 × 20 mL), basified (pH > 10) with 2 N NaOH, and extracted with CHCl<sub>3</sub> (2 × 50 mL). The combined chloroformed layers were dried (Na<sub>2</sub>SO<sub>4</sub>) and concentrated in vacuo to yield the title compound as a pale-brown powder (50 mg, quant); mp 206–210 °C. <sup>1</sup>H NMR (300 MHz, CDCl<sub>3</sub>) δ 2.11 (s, 3H), 3.68 (s, 2H), 3.69 (s, 3H), 3.95 (d, 1H, *J* = 14.3 Hz), 5.88 (d, 1H, *J* = 14.7 Hz), 6.65 (m, 2H), 6.76–7.08 (m, 6H), 7.08–7.43 (m, 3H). <sup>13</sup>C NMR (50 MHz, CDCl<sub>3</sub>) δ 18.6, 34.8, 43.3, 43.5, 101.1, 119.1, 122.1, 125.7, 128.3, 123.0, 130.2, 130.6, 133.0, 134.1, 134.9, 136.2, 138.1, 139.6, 142.5, 169.5. IR (KBr) ν (cm<sup>-1</sup>) 3361, 3286, 3193, 3070, 2941, 2868, 1629, 1608, 1561, 1504, 1447, 1413, 1387, 1380, 1317, 1298, 1252, 1176, 1138, 993, 838, 817, 756. MS (ES) *m/z* 348.25 ([M + H]<sup>+</sup>), 695.47 ([2M + H]<sup>+</sup>).

**(2S)-N-{2-Methyl-4-[(1-methyl-4,10-dihydropyrazolo[3,4-*b*]-[1,5]benzodiazepin-5(1*H*)-yl]carbonyl]benzyl}-2-[(4-methyl-1,4-diazepan-1-yl)carbonothioyl] pyrrolidine-1-carboxamide, Bis-(trifluoroacetate) (1 · 2TFA).** To a stirred solution of **10** (152 mg, 0.439 mmol) and DIEA (76 μL, 0.439 mmol) in dry DMF (3 mL) was added CDI (98 mg, 0.606 mmol). The resulting reaction mixture was stirred at rt for 1 h under argon and then treated with a solution of **11** (91 mg, 0.399 mmol) and DIEA (76 μL, 0.439 mmol) in dry DMF (1 mL). Stirring was continued at rt overnight. As TLC showed still presence of some starting amine **11**, an additional amount of activated **10** was prepared (42 mg, 0.120 mmol) and added to the reaction mixture. Stirring was continued at rt for 9 h, and then the solvent was removed in vacuo. Flash chromatography (98:1:1 to 94:5:1 CHCl<sub>3</sub>/MeOH/NH<sub>4</sub>OH) afforded an oil that was further purified by semipreparative HPLC and lyophilized to yield the title compound as a white crystalline powder (193 mg, 58%); mp 160–164 °C. [ $\alpha$ ]<sub>D</sub><sup>22</sup> +72 (*c* = 1, MeOH). <sup>1</sup>H NMR (300 MHz, DMSO-*d*<sub>6</sub>) δ 1.70–2.00 (m, 2H), 2.00–2.37 (m, including s at 2.09 ppm, 6H), 2.67–2.90 (m, 2H), 3.22 (m, 1H), 3.30–3.44 (m, 4H), 3.78 (s, 3H), 3.88 (d, 1H, *J* = 14.7 Hz), 4.08 (m, 2H), 4.38–5.10 (m, 8H), 5.67 (d, 1H, *J* = 14.7 Hz), 6.60–6.80 (m, 2H), 6.80–7.07 (m, 3H), 7.11 (t, 1H, *J* = 7.0 Hz), 7.20 (s, 1H), 7.29 (d, 1H, *J* = 7.9 Hz), 8.67 (bs, 1H). <sup>13</sup>C NMR (50 MHz, CD<sub>3</sub>OD) δ 19.7, 26.2, 27.2, 33.2, 36.0, 43.5, 45.3, 46.0, 47.0, 51.7, 52.5, 53.8, 54.0, 54.5, 56.1, 56.7, 57.2, 65.2, 104.7, 122.2, 124.9, 127.4 (m), 130.9, 131.3, 132.4, 135.5, 136.1, 136.3, 137.1, 140.1, 142.3, 144.6, 144.8, 159.5, 172.5, 209.8, 210.0. IR (KBr) ν (cm<sup>-1</sup>) 3367, 3210, 3092, 2958, 2874, 2672, 1683, 1645, 1635, 1564, 1558, 1502, 1454, 1417, 1393, 1382, 1317, 1202, 1183, 1136, 834, 797, 761, 721, 705. HRMS (ES): calcd for C<sub>32</sub>H<sub>41</sub>N<sub>8</sub>O<sub>2</sub>S, 601.3068; found, 601.3071. RP-HPLC (gradient 1): *t*<sub>R</sub> 20.3 min, purity > 98%. Anal. (C<sub>32</sub>H<sub>40</sub>N<sub>8</sub>O<sub>2</sub>S · 2C<sub>2</sub>H<sub>5</sub>F<sub>3</sub>O<sub>2</sub> · 2H<sub>2</sub>O) C, H, N: calcd, 50.00, 5.36, 12.96; found 49.90, 5.09, 12.99.

**N-{2-Methyl-4-[(1-methyl-4,10-dihydropyrazolo[3,4-*b*][1,5]benzodiazepin-5(1*H*)-yl] carbonyl]benzyl}pyrrolidine-1-carboxamide (12a).** Prepared from compound **10** (193 mg, 0.555 mmol) and pyrrolidine (51 μL, 0.610 mmol) as described for compound **1** and purified by flash chromatography (96:3:1 CHCl<sub>3</sub>/MeOH/Et<sub>3</sub>N); white powder (189 mg, 77%); mp 253–255 °C (from EtOH). <sup>1</sup>H NMR (300 MHz, DMSO-*d*<sub>6</sub>) δ 1.78 (app t, 4H, *J* = 6.2 Hz), 2.11 (s, 3H), 3.21 (app t, 4H, *J* = 6.2 Hz), 3.77 (s, 3H), 3.88 (d, 1H, *J* = 14.3 Hz), 4.09 (app d, 2H, *J* = 5.0 Hz), 5.68 (d, 1H, *J* = 14.3 Hz), 6.48 (bt, 1H, *J* = 5.6 Hz), 6.65 (t, 1H, *J* = 7.3 Hz), 6.72 (d, 1H, *J* = 7.2 Hz), 6.92 (AB system, 2H, *J* = 7.8, 7.8 Hz), 7.00 (s, 1H), 7.11 (t, 1H, *J* = 7.6 Hz), 7.16 (s, 1H), 7.28 (d, 1H, *J* = 7.8 Hz), 8.59 (bs, 1H). <sup>13</sup>C NMR (75 MHz, DMSO-*d*<sub>6</sub>) δ 18.4, 25.0, 35.3, 40.7, 43.2, 45.3, 100.3, 119.5, 121.3, 124.7, 125.4, 128.2, 129.0, 130.3, 132.6, 134.1, 134.2, 135.6, 138.9, 139.8, 140.4, 156.4, 168.1. IR (KBr) ν (cm<sup>-1</sup>) 3349, 3266, 3065, 2971, 2870, 1624, 1560, 1541, 1505, 1456, 1417, 1396, 1379, 1354, 1315, 1300, 1257, 1175, 990, 840, 815, 763, 730. HRMS (ES): calcd for C<sub>25</sub>H<sub>29</sub>N<sub>6</sub>O<sub>2</sub>, 445.2347; found, 445.2344. RP-HPLC (gradient 1): *t*<sub>R</sub> 18.4 min, purity > 98%.

**N,N-Dimethyl-N'-(2-methyl-4-[(1-methyl-4,10-dihydropyrazolo[3,4-*b*][1,5]benzodiazepin-5(1*H*)-yl]carbonyl]benzyl)urea (12b).** Prepared from compound **10** (192 mg, 0.554 mmol) and

dimethylamine hydrochloride (50 mg, 0.609 mmol) as described for compound **1** and purified by flash chromatography (98:1:1 to 96:3:1 CHCl<sub>3</sub>/MeOH/NH<sub>4</sub>OH); white foam (189 mg, 82%); mp 127–130 °C. <sup>1</sup>H NMR (300 MHz, DMSO-*d*<sub>6</sub>) δ 2.11 (s, 3H), 2.79 (s, 6H), 3.77 (s, 3H), 3.88 (d, 1H, *J* = 14.7 Hz), 4.08 (app d, 2H, *J* = 5.0 Hz), 5.67 (d, 1H, *J* = 14.4 Hz), 6.60–6.77 (m, 3H), 6.90 (AB system, 2H, *J* = 8.4, 7.8 Hz), 6.99 (s, 1H), 7.11 (t, 1H, *J* = 7.5 Hz), 7.16 (s, 1H), 7.28 (d, 1H, *J* = 8.1 Hz), 8.59 (bs, 1H). <sup>13</sup>C NMR (75 MHz, DMSO-*d*<sub>6</sub>) δ 18.4, 35.3, 35.9, 41.0, 43.2, 100.3, 119.5, 121.3, 124.7, 125.3, 128.2, 129.1, 130.3, 132.6, 134.1, 134.3, 135.6, 138.9, 139.8, 140.4, 158.0, 168.1. IR (KBr) ν (cm<sup>-1</sup>) 3389, 3125, 3031, 2941, 2863, 2823, 1624, 1558, 1538, 1506, 1488, 1449, 1417, 1379, 1320, 1259, 1230, 1064, 839, 759, 730, 663, 618. HRMS (ES): calcd for C<sub>23</sub>H<sub>27</sub>N<sub>6</sub>O<sub>2</sub>, 419.2190; found, 419.2186. RP-HPLC (gradient 1): *t*<sub>R</sub> 17.5 min, purity > 95%.

**N-{2-Methyl-4-[(1-methyl-4,10-dihydropyrazolo[3,4-*b*][1,5]benzodiazepin-5(1*H*)-yl] carbonyl]benzyl}acetamide (12c).** To a stirred solution of **10** (177 mg, 0.509 mmol) and Et<sub>3</sub>N (106 μL, 0.763 mmol) in dry DCM (4 mL) was added Ac<sub>2</sub>O (53 μL, 0.560 mmol). Stirring was continued at rt for 3 h under argon. The reaction mixture was diluted with DCM (10 mL), and the organic layer was separated, washed with 10% citric acid (5 mL) and satd NaHCO<sub>3</sub> (5 mL). The aqueous phases were basified with 10 N NaOH and extracted with CHCl<sub>3</sub> (2 × 20 mL). The combined organic layers were dried (Na<sub>2</sub>SO<sub>4</sub>) and concentrated in vacuo. Flash chromatography (95:4:1 to 90:8:2 AcOEt/MeOH/Et<sub>3</sub>N) afforded the title compound as a white powder (75 mg, 38%); mp 218–220 °C (from EtOH/AcOEt). <sup>1</sup>H NMR (300 MHz, DMSO-*d*<sub>6</sub>) δ 1.84 (s, 3H), 2.11 (s, 3H), 3.77 (s, 3H), 3.89 (d, 1H, *J* = 14.7 Hz), 4.12 (app d, 2H, *J* = 2.8 Hz), 5.67 (d, 1H, *J* = 14.3 Hz), 6.65 (t, 1H, *J* = 7.3 Hz), 6.72 (d, 1H, *J* = 7.2 Hz), 6.89 (AB system, 2H, *J* = 7.8, 7.8 Hz), 7.04 (s, 1H), 7.11 (t, 1H, *J* = 7.6 Hz), 7.17 (s, 1H), 7.29 (d, 1H, *J* = 8.1 Hz), 8.16 (app t, 1H), 8.61 (bs, 1H). <sup>13</sup>C NMR (75 MHz, DMSO-*d*<sub>6</sub>) δ 18.4, 22.4, 35.3, 43.1, 100.3, 119.5, 121.3, 124.8, 126.1, 128.2, 129.3, 130.3, 132.5, 134.7, 134.9, 135.6, 138.6, 138.9, 139.8, 167.9, 169.1. IR (KBr) ν (cm<sup>-1</sup>) 3311, 3294, 3081, 2964, 2919, 1622, 1610, 1564, 1507, 1449, 1420, 1385, 1299, 1262, 1250, 1175, 1025, 996, 836, 816, 768, 750, 730. HRMS (ES): calcd for C<sub>22</sub>H<sub>24</sub>N<sub>5</sub>O<sub>2</sub>, 390.1925; found, 390.1922. RP-HPLC (gradient 1): *t*<sub>R</sub> 17.0 min, purity > 98%.

**Methyl 2-Chloro-4-nitrobenzoate (17).** A solution of 2-chloro-4-nitrobenzoyle chloride **16** (1.020 g, 4.64 mmol) in dry MeOH (5 mL) was stirred at 0 °C for 5 min and then allowed to warm to rt and stirring was continued for 2 h. The solvent was removed in vacuo and the residue dried under high vacuum to yield the title compound as a white powder (1.086 g, quant); mp 62–64 °C. <sup>1</sup>H NMR (200 MHz, CDCl<sub>3</sub>) δ 3.99 (s, 3H), 7.97 (d, 1H, *J* = 8.3 Hz), 8.16 (dd, 1H, *J* = 8.6, 2.2 Hz), 8.31 (s, 1H). <sup>13</sup>C NMR (75 MHz, CDCl<sub>3</sub>) δ 53.1, 121.4, 126.0, 132.0, 134.8, 135.7, 149.4, 164.6. IR (KBr) ν (cm<sup>-1</sup>) 3098, 3031, 2964, 1721, 1589, 1527, 1430, 1387, 1358, 1299, 1245, 1189, 1129, 1043, 945, 890, 853, 825, 780, 758, 742.

**Methyl 4-Amino-2-chlorobenzoate (18).** A mixture of **17** (974 mg, 4.52 mmol) and SnCl<sub>2</sub> · 2H<sub>2</sub>O (5.10 g, 22.60 mmol) in EtOH (50 mL) was refluxed under argon. After 1 h, the reaction mixture was cooled to 0 °C and 1 N NaHCO<sub>3</sub> was added slowly until pH 7–8 (65 mL). The resulting milky mixture was stirred at rt for 1 h, and then the solvent was removed in vacuo and the resulting aqueous phase was extracted with AcOEt (200 mL). The organic layer was washed with brine (50 mL), and the aqueous phase was extracted with DCM (200 mL). The combined organic layers were dried (Na<sub>2</sub>SO<sub>4</sub>) and concentrated in vacuo to yield the title compound as an orange crystalline solid (928 mg, quant); mp 100–102 °C. <sup>1</sup>H NMR (200 MHz, CDCl<sub>3</sub>) δ 3.85 (s, 3H), 3.96 (bs, 2H), 6.52 (dd, 1H, *J* = 8.5, 2.2 Hz), 6.69 (d, 1H, *J* = 2.2 Hz), 7.76 (d, 1H, *J* = 8.6 Hz). <sup>13</sup>C NMR (75 MHz, CDCl<sub>3</sub>) δ 51.8, 112.3, 116.3, 118.0, 133.8, 136.1, 150.5, 165.7. IR (KBr) ν (cm<sup>-1</sup>) 3427, 3333, 3003, 2952, 1703, 1633, 1598, 1550, 1499, 1429, 1329, 1264, 1248, 1186, 1122, 1040, 906, 862, 850, 831, 773, 685.

**Methyl 2-Chloro-4-cyanobenzoate (19).** A suspension of **18** (510 mg, 2.75 mmol) in conc HCl (5.5 mL) was cooled to  $-15^{\circ}\text{C}$  and ice (30 mL) was added. Then a solution of  $\text{NaNO}_2$  (235 mg, 3.30 mmol) in water (5 mL) was added dropwise under argon. The resulting reaction mixture was stirred at  $-15^{\circ}\text{C}$  for 15 min. The presence of  $\text{HNO}_2$  excess was checked with a starch-iodide paper. The mixture was then carefully neutralized by adding solid  $\text{Na}_2\text{CO}_3$  with constant stirring (pH 5). At  $-10^{\circ}\text{C}$ , a mixture of KCN (497 mg, 6.87 mmol) and CuCN (320 mg, 3.57 mmol) in cold water (8 mL) was added dropwise. Stirring was continued for 2 h from  $-10^{\circ}\text{C}$  to rt. The reaction mixture was then filtered and extracted with DCM ( $2 \times 75$  mL). The combined organic layers were dried ( $\text{Na}_2\text{SO}_4$ ) and concentrated in vacuo. Flash chromatography (95:5 *n*-heptane/AcOEt) afforded the title compound as a white woolly solid (328 mg, 61%); mp  $76-80^{\circ}\text{C}$ .  $^1\text{H}$  NMR (200 MHz,  $\text{CDCl}_3$ )  $\delta$  3.97 (s, 3H), 7.61 (dd, 1H,  $J = 8.1, 1.5$  Hz), 7.75 (d, 1H,  $J = 1.5$  Hz), 7.90 (d, 1H,  $J = 8.1$  Hz).  $^{13}\text{C}$  NMR (50 MHz,  $\text{CDCl}_3$ )  $\delta$  53.0, 116.2, 116.6, 130.0, 131.8, 132.2, 134.3, 134.6, 164.7. IR (KBr)  $\nu$  ( $\text{cm}^{-1}$ ) 3070, 3048, 2969, 2235, 1722, 1435, 1387, 1306, 1295, 1259, 1194, 1136, 1054, 954, 895, 845, 805, 775, 607.

**2-Chloro-4-cyanobenzoic Acid (20).** A solution of **19** (967 mg, 4.94 mmol) and  $\text{LiOH}\cdot\text{H}_2\text{O}$  (318 mg, 7.41 mmol) in a 1:1 MeOH/THF mixture (10 mL) was stirred at rt for 1 h. The solvent was removed in vacuo, and then the resulting residue was taken up with water (10 mL) and acidified with 6 N HCl (pH 1). The precipitate was filtered and dried under vacuum over  $\text{P}_2\text{O}_5$  and then at  $45^{\circ}\text{C}$  for 8 h to yield the title compound as a pale-pink powder (744 mg, 83%); mp  $160-162^{\circ}\text{C}$ .  $^1\text{H}$  NMR (300 MHz,  $\text{DMSO}-d_6$ )  $\delta$  7.90 (m, 2H), 8.16 (s, 1H), 14.01 (bs, 1H).  $^{13}\text{C}$  NMR (50 MHz,  $\text{DMSO}-d_6$ )  $\delta$  114.6, 116.8, 130.9, 131.1, 131.8, 133.8, 136.3, 165.7. IR (KBr)  $\nu$  ( $\text{cm}^{-1}$ ) 3300–2400, 3076, 3048, 2235, 1717, 1687, 1600, 1544, 1485, 1429, 1408, 1383, 1302, 1261, 1054, 903, 884, 848, 778, 683. MS (ES)  $m/z$  179.97 ( $[\text{M} - \text{H}]^-$ ).

**2-Methyl-4-(2,3,4,5-tetrahydro-1H-1-benzazepin-1-ylcarbonyl)benzoxazine (21a).** The acyl chloride of the acid **8** (301 mg, 1.87 mmol) was prepared according to the procedure described for compound **9**. It was then dissolved in dry DCM (2 mL), and this mixture was added dropwise, under argon, to a stirred ice-cold solution of **13** (250 mg, 1.70 mmol), anhydrous pyridine (0.41 mL, 5.10 mmol), and DMAP (6.2 mg, 0.05 mmol) in dry DCM (4 mL). Stirring was continued at  $0^{\circ}\text{C}$  for 30 min then at rt overnight. The reaction mixture was diluted in DCM (40 mL), washed with 1 N HCl (5 mL) and satd  $\text{NaHCO}_3$  (5 mL), dried ( $\text{Na}_2\text{SO}_4$ ), and concentrated in vacuo. Flash chromatography (8:2 *n*-heptane/AcOEt) afforded the title compound as a white powder (375 mg, 76%); mp  $126-128^{\circ}\text{C}$ .  $^1\text{H}$  NMR (300 MHz,  $\text{CDCl}_3$ )  $\delta$  1.40–1.70 (m, 1H), 1.90–2.20 (m, 3H), 2.41 (s, 3H), 2.70–3.10 (m, 3H), 4.96 (app bd, 1H,  $J = 13.1$  Hz), 6.59 (d, 1H,  $J = 7.5$  Hz), 6.87–6.97 (m, 2H), 7.10 (dt, 1H,  $J = 7.5, 0.9$  Hz), 7.19–7.27 (m, 2H), 7.31 (d, 1H,  $J = 7.8$  Hz).  $^{13}\text{C}$  NMR (75 MHz,  $\text{CDCl}_3$ )  $\delta$  20.3, 26.3, 29.5, 34.9, 47.8, 113.4, 117.5, 125.4, 127.1, 127.7, 128.2, 129.8, 130.2, 131.7, 139.3, 140.5, 141.7, 143.1, 167.4. IR (KBr)  $\nu$  ( $\text{cm}^{-1}$ ) 3059, 2930, 2851, 2222, 1644, 1603, 1578, 1558, 1492, 1438, 1413, 1384, 1359, 1317, 1274, 895, 851, 828, 775, 759, 741.

**2-Methyl-4-(5H-pyrrolo[2,1-c][1,4]benzodiazepin-10(11H)-ylcarbonyl)benzoxazine (21b).** Prepared from acid **8** (304 mg, 1.79 mmol) and amine **14** (300 mg, 1.63 mmol) as described for compound **21a** (without DMAP); pale-yellow powder (345 mg, 65%); mp  $186-188^{\circ}\text{C}$ .  $^1\text{H}$  NMR (300 MHz,  $\text{CDCl}_3$ )  $\delta$  2.46 (s, 3H), 5.19 (app bs, 4H), 6.06 (m, 1H), 6.10 (t, 1H,  $J = 3.0$  Hz), 6.71 (m, 1H), 6.78 (m, 1H), 6.93–7.16 (m, 2H), 7.20 (t, 1H,  $J = 7.3$  Hz), 7.32–7.50 (m, 3H).  $^{13}\text{C}$  NMR (75 MHz,  $\text{CDCl}_3$ )  $\delta$  20.4, 46.4, 51.2, 107.8, 108.7, 114.1, 117.3, 121.9, 125.6, 125.8, 128.1, 129.0, 129.5, 130.1, 131.9, 134.1, 139.4, 141.7, 142.4, 168.5. IR (ATR)  $\nu$  ( $\text{cm}^{-1}$ ) 2921, 2854, 2229, 1644, 1584, 1492, 1462, 1447, 1407, 1368, 1301, 1270, 1246, 1214, 1199, 1076, 890, 853, 841, 827, 757, 728, 701, 682, 612. MS (ES)  $m/z$  328.1 ( $[\text{M} + \text{H}]^+$ ), 350.1 ( $[\text{M} + \text{Na}]^+$ ).

**3-Chloro-4-(5H-pyrrolo[2,1-c][1,4]benzodiazepin-10(11H)-ylcarbonyl)benzoxazine (21c).** The acyl chloride of the acid **20** (25 mg, 0.138 mmol) was prepared according to the procedure described for compound **9**. It was then dissolved in dry DCM (0.3 mL), and this mixture was added dropwise, under argon, to a stirred ice-cold solution of **14** (21 mg, 0.115 mmol), anhydrous pyridine (28  $\mu\text{L}$ , 0.345 mmol), and DMAP (0.4 mg, 0.003 mmol) in dry DCM (0.3 mL). The reaction mixture was irradiated under microwaves at  $80^{\circ}\text{C}$  (1 bar) for 6 min and then diluted in DCM (15 mL), washed with 1 N HCl (3 mL) and satd  $\text{NaHCO}_3$  (3 mL), dried ( $\text{Na}_2\text{SO}_4$ ), and concentrated in vacuo. Flash chromatography (8:2 to 7:3 *n*-heptane/AcOEt) afforded the title compound as a white powder (20 mg, 49%); mp  $104-106^{\circ}\text{C}$ .  $^1\text{H}$  NMR (300 MHz,  $\text{DMSO}-d_6$ )  $\delta$  4.90–5.50 (m, 4H), 5.90 (t, 1H,  $J = 3.0$  Hz), 6.01 (m, 1H), 6.83 (app t, 1H,  $J = 1.9$  Hz), 7.00–7.10 (m, 2H), 7.10–7.18 (m, 1H), 7.40 (d, 1H,  $J = 7.2$  Hz), 7.45–7.65 (m, 1H), 7.69 (d, 1H,  $J = 7.5$  Hz), 7.99 (s, 1H).  $^{13}\text{C}$  NMR (75 MHz,  $\text{DMSO}-d_6$ )  $\delta$  45.1, 49.2, 106.8, 108.7, 113.0, 116.9, 122.3, 124.6, 125.0, 128.1, 128.6, 128.8, 129.6, 130.8, 132.9, 135.7, 139.1, 140.6, 165.3. IR (KBr)  $\nu$  ( $\text{cm}^{-1}$ ) 3098, 3064, 2952, 2919, 2852, 2230, 1653, 1600, 1580, 1493, 1390, 1371, 1351, 1303, 1273, 1194, 834, 758, 714, 686, 612.

**2-Methyl-4-[[4-(2-oxo-2H-3,1-benzoxazin-1(4H)-yl)piperidin-1-yl]carbonyl]benzoxazine (21d).** To a solution of **15** (288 mg, 1.62 mmol) in dry DMF (6 mL) were added successively EDCI·HCl (381 mg, 1.95 mmol), HOBT· $\text{H}_2\text{O}$  (269 mg, 1.95 mmol), **8** (377 mg, 1.78 mmol), and then DIEA (0.56 mL, 3.25 mmol) dropwise. Stirring was continued at rt for 14 h, and then the solvent was removed in vacuo. The resulting residue was taken up in AcOEt (50 mL). This organic layer was washed with 10% citric acid (20 mL), satd  $\text{NaHCO}_3$  (20 mL) and brine (20 mL), dried ( $\text{Na}_2\text{SO}_4$ ), and concentrated in vacuo. Flash chromatography (5:5 to 3:7 *n*-heptane/AcOEt) afforded the title compound as a white foam (394 mg, 65%); mp  $64-68^{\circ}\text{C}$ .  $^1\text{H}$  NMR (300 MHz,  $\text{CDCl}_3$ )  $\delta$  1.75–2.10 (m, 2H), 2.58 (s, 3H), 2.60–3.00 (m, 3H), 3.13 (m, 1H), 3.80 (m, 1H), 4.00–4.20 (m, 1H), 4.92 (m, 1H), 5.10 (s, 2H), 7.00–7.24 (m, 3H), 7.30–7.50 (m, 3H), 7.65 (d, 1H,  $J = 7.9$  Hz).  $^{13}\text{C}$  NMR (50 MHz,  $\text{CDCl}_3$ )  $\delta$  20.5, 28.0, 28.8, 42.1, 47.3, 56.4, 67.1, 113.3, 113.9, 117.4, 122.4, 123.4, 124.5, 125.0, 128.6, 129.2, 132.7, 138.6, 140.1, 142.7, 152.5, 168.5. IR (KBr)  $\nu$  ( $\text{cm}^{-1}$ ) 3048, 2975, 2934, 2870, 2226, 1716, 1633, 1607, 1498, 1468, 1454, 1447, 1389, 1293, 1273, 1258, 1242, 1204, 1042, 771, 755.

**1-[2-Methyl-4-(2,3,4,5-tetrahydro-1H-1-benzazepin-1-ylcarbonyl)phenyl]methanamine (22a).** Prepared from compound **21a** (367 mg, 1.26 mmol) as described for compound **10**; cream-colored powder (329 mg, 89%); mp  $96-98^{\circ}\text{C}$ .  $^1\text{H}$  NMR (300 MHz,  $\text{CDCl}_3$ )  $\delta$  1.30–2.20 (m, 4H), 2.16 (s, 3H), 2.50–3.10 (m, 3H), 3.73 (s, 2H), 5.00 (app bd, 1H,  $J = 12.8$  Hz), 6.62 (d, 1H,  $J = 7.8$  Hz), 6.75–6.92 (m, 2H), 6.95–7.08 (m, 2H), 7.11 (s, 1H), 7.20 (d, 1H,  $J = 7.2$  Hz).  $^{13}\text{C}$  NMR (75 MHz,  $\text{CDCl}_3$ )  $\delta$  18.6, 26.3, 29.6, 34.9, 43.5, 47.6, 125.8, 126.9, 127.0, 128.2, 129.8, 130.2, 134.5, 135.0, 139.2, 142.1, 142.2, 144.1, 168.9. IR (KBr)  $\nu$  ( $\text{cm}^{-1}$ ) 3379, 3316, 3064, 3045, 2942, 2924, 2879, 2840, 1633, 1578, 1564, 1492, 1456, 1435, 1411, 1377, 1356, 1312, 1276, 1259, 1209, 1166, 1052, 1033, 967, 889, 862, 819, 761, 755.

**1-[2-Methyl-4-(5H-pyrrolo[2,1-c][1,4]benzodiazepin-10(11H)-ylcarbonyl)phenyl]methanamine (22b).** Prepared from compound **21b** (259 mg, 0.790 mmol) as described for compound **10**; pale-brown foam (32 mg, 12%); mp  $62-66^{\circ}\text{C}$ .  $^1\text{H}$  NMR (300 MHz,  $\text{CDCl}_3$ )  $\delta$  2.22 (s, 3H), 3.80 (s, 2H), 5.20 (app bs, 4H), 6.04 (s, 1H), 6.09 (t, 1H,  $J = 3.1$  Hz), 6.69 (s, 1H), 6.87 (m, 1H), 6.99 (m, 1H), 7.04–7.21 (m, 3H), 7.24 (m, 1H), 7.36 (d, 1H,  $J = 7.2$  Hz).  $^{13}\text{C}$  NMR (75 MHz,  $\text{CDCl}_3$ )  $\delta$  18.7, 43.5, 46.5, 51.3, 107.5, 108.1, 121.5, 126.0, 126.5, 127.4, 128.7, 128.9, 129.3, 130.4, 133.5, 134.0, 135.4, 142.9, 170.2. IR (ATR)  $\nu$  ( $\text{cm}^{-1}$ ) 3369, 3306, 2920, 2851, 1650, 1640, 1634, 1583, 1574, 1568, 1493, 1454, 1446, 1408, 1366, 1348, 1303, 1271, 1188, 1148, 1075, 825, 755, 745, 710, 611. MS (ES)  $m/z$  332.2 ( $[\text{M} + \text{H}]^+$ ).

**1-[3-Chloro-4-(5H-pyrrolo[2,1-c][1,4]benzodiazepin-10(11H)-ylcarbonyl)phenyl]methanamine (22c).** Prepared from compound

**21c** (207 mg, 0.594 mmol) as described for compound **10**; pale-yellow gum (64 mg, 30%). <sup>1</sup>H NMR (300 MHz, CDCl<sub>3</sub>) δ 3.70–4.05 (m, 2H), 5.00–5.40 (m, 4H), 5.95–6.15 (m, 2H), 6.60–6.70 (m, 1H), 6.85–7.18 (m, 4H), 7.18–7.60 (m, 3H). <sup>13</sup>C NMR (75 MHz, CDCl<sub>3</sub>) δ 45.6, 51.1, 51.3, 107.6, 108.9, 121.8, 125.7, 125.8, 127.7, 127.9, 128.0, 128.2, 128.4, 128.6, 128.9, 129.0, 131.1, 134.6, 134.8, 140.4, 148.8, 167.8. IR (CsI) ν (cm<sup>-1</sup>) 3383, 3042, 2919, 2852, 1652, 1606, 1495, 1398, 1306, 1274, 758, 718.

**1-[(2-Methyl-4-[(4-(2-oxo-2H-3,1-benzoxazin-1(4H)-yl)piperidin-1-yl)carbonyl]phenyl)methanamine (22d)**. Prepared from compound **21d** (338 mg, 0.90 mmol) as described for compound **10**; beige powder (188 mg, 55%); mp 128–130 °C. <sup>1</sup>H NMR (200 MHz, DMSO-*d*<sub>6</sub>) δ 1.50–2.00 (m, 2H), 2.00–2.35 (m, 3H), 2.55–4.80 (m, 9H), 4.80–5.20 (m, 2H), 6.80–7.50 (m, 7H). <sup>13</sup>C NMR (50 MHz, DMSO-*d*<sub>6</sub>) δ 18.5, 28.4, 46.6, 55.3, 66.3, 114.0, 122.6, 123.0, 124.1, 124.8, 128.2, 128.4, 129.1, 135.5, 136.7, 138.6, 151.8, 168.8. IR (KBr) ν (cm<sup>-1</sup>) 2963, 2934, 2863, 1719, 1709, 1607, 1564, 1499, 1467, 1446, 1390, 1303, 1292, 1259, 1206, 1111, 1041, 769, 755, 620. MS (ES) *m/z* 380.24 ([M + H]<sup>+</sup>).

**(2S)-N-[2-Methyl-4-(2,3,4,5-tetrahydro-1H-1-benzazepin-1-ylcarbonyl)benzyl]-2-[(4-methyl-1,4-diazepan-1-yl)carbonothioyl]pyrrolidine-1-carboxamide (23a)**. Prepared from compound **22a** (159 mg, 0.539 mmol) and compound **11** (88 mg, 0.385 mmol) as described for compound **1** and purified by flash chromatography (CHCl<sub>3</sub>/Et<sub>3</sub>N 0.7 to 2%). White foam (199 mg, 95%); mp 98–100 °C; [α]<sub>D</sub><sup>22</sup> -67 (*c* = 1, CHCl<sub>3</sub>). <sup>1</sup>H NMR (300 MHz, DMSO-*d*<sub>6</sub>) δ 1.30–1.50 (m, 1H), 1.60–2.22 (m, 9H), 2.25 (s, 3H), 2.35–2.78 (m, 4H), 2.80–3.10 (m, 3H), 3.16–3.50 (m, 4H), 3.50–3.64 (m, 1H), 3.72–4.30 (m, 6H), 4.83 (app bd, 1H, *J* = 13.1 Hz), 4.96 (m, 1H), 6.48 (bs, 1H), 6.68 (d, 1H, *J* = 7.5 Hz), 6.80 (app bt, 1H, *J* = 9.0 Hz), 6.87–7.13 (m, 4H), 7.28 (d, 1H, *J* = 7.5 Hz). <sup>13</sup>C NMR (75 MHz, DMSO-*d*<sub>6</sub>) δ 18.4, 23.6, 24.6, 25.9, 26.6, 29.3, 31.3, 34.2, 45.3, 45.5, 45.6, 46.1, 46.2, 47.0, 49.9, 50.8, 53.0, 53.2, 54.9, 55.4, 55.8, 57.0, 61.9, 62.0, 124.6, 124.8, 125.2, 125.4, 126.9, 127.0, 128.1, 129.0, 129.8, 134.1, 134.2, 139.1, 140.2, 143.9, 155.5, 167.9, 205.0, 205.2. IR (KBr) ν (cm<sup>-1</sup>) 3328, 2939, 2863, 2801, 1634, 1540, 1505, 1492, 1456, 1438, 1415, 1393, 1379, 1354, 1314, 1202, 1138, 1032, 755, 744. HRMS (ES): calcd for C<sub>31</sub>H<sub>42</sub>N<sub>5</sub>O<sub>2</sub>S, 548.3054; found, 548.3054. RP-HPLC (gradient 1): *t*<sub>R</sub> 20.8 min, purity > 98%.

**(2S)-N-[2-Methyl-4-(5H-pyrrolo[2,1-*c*][1,4]benzodiazepin-10(11H)-ylcarbonyl)benzyl]-2-[(4-methyl-1,4-diazepan-1-yl)carbonothioyl]pyrrolidine-1-carboxamide, Trifluoroacetate (23b·TFA)**. Prepared from compound **22b** (32 mg, 0.096 mmol) and compound **11** (24 mg, 0.106 mmol) as described for compound **1** and purified by flash chromatography (98:1:1 to 94:5:1 CHCl<sub>3</sub>/MeOH/NH<sub>4</sub>OH) followed by semipreparative HPLC; white hygroscopic powder (29 mg, 51%); mp 140–142 °C; [α]<sub>D</sub><sup>22</sup> +17 (*c* = 0.1, MeOH). <sup>1</sup>H NMR (300 MHz, CDCl<sub>3</sub>) δ 1.83–2.10 (m, 5H), 2.20 (s, 3H), 2.38 (d, 3H, *J* = 4.3 Hz), 2.47–2.92 (m, 4H), 3.34–3.48 (m, 1H), 3.58–3.72 (m, 1H), 3.75–4.22 (m, 4H), 4.22–4.55 (m, 4H), 5.03–5.30 (m, 4H), 6.03 (s, 1H), 6.09 (app t, 1H, *J* = 2.8 Hz), 6.69 (s, 1H), 6.88 (m, 1H), 7.01 (m, 1H), 7.06–7.23 (m, 4H), 7.36 (d, 1H, *J* = 7.2 Hz). <sup>13</sup>C NMR (75 MHz, CDCl<sub>3</sub>) δ 18.9, 24.0, 24.1, 27.1, 29.7, 31.7, 31.8, 42.2, 46.3, 46.4, 46.6, 50.6, 51.0, 51.3, 53.6, 54.0, 55.7, 55.9, 56.8, 57.8, 62.6, 62.9, 107.5, 108.0, 121.5, 121.8, 125.9, 126.5, 126.7, 127.6, 128.7, 128.9, 129.4, 130.4, 133.9, 135.9, 139.5, 142.8, 156.0, 170.1, 204.9, 205.6. IR (ATR) ν (cm<sup>-1</sup>) 3367, 2953, 2874, 2725, 2678, 1644, 1633, 1614, 1548, 1538, 1495, 1416, 1372, 1351, 1304, 1274, 1197, 1172, 1137, 796, 753, 717, 704, 593. HRMS (ES): calcd for C<sub>33</sub>H<sub>41</sub>N<sub>6</sub>O<sub>2</sub>S, 585.3006; found, 585.3002. RP-HPLC (gradient 2): *t*<sub>R</sub> 18.8 min, purity > 98%.

**(2S)-N-[3-Chloro-4-(5H-pyrrolo[2,1-*c*][1,4]benzodiazepin-10(11H)-ylcarbonyl)benzyl]-2-[(4-methyl-1,4-diazepan-1-yl)carbonothioyl]pyrrolidine-1-carboxamide (23c)**. Prepared from compound **22c** (55 mg, 0.157 mmol) and compound **11** (39 mg, 0.173 mmol) as described for compound **1** and purified by flash chromatography (CHCl<sub>3</sub>/Et<sub>3</sub>N 1 to 2%); cream powder (83 mg, 87%); mp 146–150 °C; [α]<sub>D</sub><sup>22</sup> -31

(*c* = 1, CHCl<sub>3</sub>). <sup>1</sup>H NMR (200 MHz, CDCl<sub>3</sub>) δ 1.80–3.10 (m, 14H, including d at 2.44 ppm, *J* = 8.4 Hz), 3.30–3.53 (m, 1H), 3.58–4.20 (m, 4H), 4.22–4.53 (m, 2H), 4.53–4.87 (m, 2H), 4.87–5.40 (m, 4H), 6.06 (m, 2H), 6.66 (m, 1H), 6.94–7.7.58 (m, 7H). <sup>13</sup>C NMR (50 MHz, CDCl<sub>3</sub>) δ 22.6, 22.9, 24.1, 24.2, 25.0, 26.4, 27.9, 29.6, 31.8, 43.4, 44.0, 45.6, 46.0, 46.5, 50.4, 50.7, 51.1, 51.3, 52.8, 53.9, 55.4, 55.7, 56.8, 57.5, 62.7, 62.9, 107.6, 108.8, 121.7, 125.2, 125.8, 126.1, 126.5, 126.7, 127.6, 128.1, 128.3, 128.8, 129.0, 131.1, 134.0, 134.5, 134.7, 140.5, 142.6, 156.1, 167.7, 205.1, 205.9. IR (KBr) ν (cm<sup>-1</sup>) 3400, 2930, 2863, 2796, 1641, 1531, 1494, 1458, 1382, 1200, 758, 716. HRMS (ES): calcd for C<sub>32</sub>H<sub>38</sub>ClN<sub>6</sub>O<sub>2</sub>S, 605.2460; found, 605.2443. RP-HPLC (gradient 1): *t*<sub>R</sub> 21.2 min, purity > 98%.

**(2S)-N-[2-Methyl-4-[(4-(2-oxo-2H-3,1-benzoxazin-1(4H)-yl)piperidin-1-yl)carbonyl]benzyl]-2-[(4-methyl-1,4-diazepan-1-yl)carbonothioyl]pyrrolidine-1-carboxamide (23d)**. Prepared from compound **22d** (150 mg, 0.396 mmol) and compound **11** (75 mg, 0.330 mmol) as described for compound **1** and purified by flash chromatography (98:1:1 to 97:2:1 CHCl<sub>3</sub>/MeOH/NH<sub>4</sub>OH); white foam (153 mg, 74%); mp 136–140 °C; [α]<sub>D</sub><sup>22</sup> +47 (*c* = 1, CHCl<sub>3</sub>). <sup>1</sup>H NMR (200 MHz, CDCl<sub>3</sub>) δ 0.60–5.20 (m, including s at 2.32 ppm and s at 5.09 ppm, 37H), 6.80–7.70 (m, 7H). <sup>13</sup>C NMR (75 MHz, CDCl<sub>3</sub>) δ 19.1, 24.4, 28.9, 31.8, 42.2, 45.5, 45.8, 45.9, 46.3, 50.0, 51.5, 53.3, 55.0, 55.4, 56.6, 62.6, 67.1, 113.5, 121.4, 122.4, 123.3, 124.4, 124.9, 127.3, 128.7, 129.2, 134.6, 134.8, 136.4, 138.6, 138.9, 152.6, 156.2, 170.5. IR (KBr) ν (cm<sup>-1</sup>) 3337, 2947, 2937, 2870, 2801, 1717, 1625, 1608, 1541, 1498, 1467, 1457, 1388, 1348, 1291, 1258, 1204, 1133, 1041, 769, 753. HRMS (ES): calcd for C<sub>34</sub>H<sub>45</sub>N<sub>6</sub>O<sub>4</sub>S, 633.3218; found, 633.3190. RP-HPLC (gradient 1): *t*<sub>R</sub> 20.1 min, purity > 98%.

**1-Methyl-5-(3-methyl-4-nitrobenzoyl)-1,4,5,10-tetrahydropyrazolo[3,4-*b*][1,5]benzodiazepine (25)**. The acyl chloride of 3-methyl-4-nitrobenzoic acid **24** (271 mg, 1.50 mmol) was prepared according to the procedure described for compound **9**. It was then dissolved in dry DCM (2 mL), and this mixture was added dropwise, under argon, to a stirred ice-cold solution of **7** (250 mg, 1.25 mmol) and Et<sub>3</sub>N (0.52 mL, 3.74 mmol) in dry DCM (3 mL). Stirring was continued at 0 °C for 30 min then at rt overnight. The reaction mixture was diluted in DCM (25 mL), washed with 10% citric acid (10 mL) and satd NaHCO<sub>3</sub> (15 mL), dried (Na<sub>2</sub>SO<sub>4</sub>), and concentrated in vacuo to yield a residue that was triturated in AcOEt. The precipitate was filtered, washed with AcOEt, and dried under high vacuum to yield the title compound as a yellow powder (409 mg, 90%); mp 222–224 °C. <sup>1</sup>H NMR (300 MHz, DMSO-*d*<sub>6</sub>) δ 2.36 (s, 3H), 3.78 (s, 3H), 3.97 (d, 1H, *J* = 14.3 Hz), 5.65 (d, 1H, *J* = 14.7 Hz), 6.66 (td, 1H, *J* = 7.8, 1.2 Hz), 6.83 (dd, 1H, *J* = 7.8, 1.6 Hz), 7.07–7.17 (m, 2H), 7.20 (s, 1H), 7.29 (dd, 1H, *J* = 8.4, 1.3 Hz), 7.32 (s, 1H), 7.74 (d, 1H, *J* = 8.4 Hz), 8.67 (bs, 1H). <sup>13</sup>C NMR (75 MHz, DMSO-*d*<sub>6</sub>) δ 19.4, 35.5, 43.4, 100.2, 119.7, 121.5, 124.0, 125.8, 129.0, 130.6, 131.5, 131.6, 132.6, 135.9, 139.2, 139.8, 141.1, 148.9, 166.8. IR (KBr) ν (cm<sup>-1</sup>) 3343, 3098, 3076, 2986, 2930, 2858, 1632, 1605, 1565, 1524, 1503, 1414, 1382, 1356, 1318, 1293, 1252, 1180, 843, 769, 734.

**2-Methyl-4-[(1-methyl-4,10-dihydropyrazolo[3,4-*b*][1,5]benzodiazepin-5(1H)-yl)carbonyl]aniline (26)**. A mixture of **25** (318 mg, 0.875 mmol) and SnCl<sub>4</sub>·2H<sub>2</sub>O (987 mg, 4.374 mmol) in EtOH (11 mL) was refluxed under argon. After 1 h, the reaction mixture was cooled to 0 °C and 1 N NaHCO<sub>3</sub> was added slowly until pH 7–8 (7 mL). The resulting mixture was stirred at rt for 1.5 h and then extracted with AcOEt (2 × 100 mL). The aqueous phase was filtered over celite to eliminate the excess of salts and extracted with AcOEt (100 mL). The combined organic layers were washed with brine (30 mL), dried (Na<sub>2</sub>SO<sub>4</sub>), and concentrated in vacuo to yield a residue that was triturated in AcOEt. The precipitate was filtered, washed with AcOEt, and dried under high vacuum to yield the title compound as a white powder (240 mg, 82%); mp 250–252 °C. <sup>1</sup>H NMR (300 MHz, DMSO-*d*<sub>6</sub>) δ 1.88 (s, 3H), 3.76 (m, 3H), 3.75–3.90 (m, 1H), 5.17 (bs, 2H), 5.66 (app bd, 1H, *J* = 14.3 Hz), 6.25 (d, 1H, *J* = 8.1 Hz), 6.67 (m, 3H), 6.88 (s, 1H), 7.12

(m, 2H), 7.29 (d, 1H,  $J = 8.1$  Hz), 8.53 (bs, 1H).  $^{13}\text{C}$  NMR (75 MHz, DMSO- $d_6$ )  $\delta$  17.2, 35.3, 43.2, 100.6, 111.9, 119.3, 119.5, 121.3, 122.4, 127.2, 127.6, 130.2, 130.8, 133.6, 135.5, 138.6, 140.0, 148.3, 168.3. IR (KBr)  $\nu$  ( $\text{cm}^{-1}$ ) 3428, 3346, 3221, 3064, 2969, 2935, 1620, 1605, 1562, 1506, 1446, 1421, 1381, 1317, 1302, 1261, 1177, 1157, 824, 755, 732, 629. MS (ES)  $m/z$  334.23 ( $[\text{M} + \text{H}]^+$ ).

**5-[4-[(1,1'-Biphenyl-2-ylcarbonyl)amino]-3-methylbenzoyl]-1-methyl-1,4,5,10-tetrahydropyrazolo[3,4-*b*][1,5]benzodiazepine (27).** Prepared from 2-phenylbenzoic acid (445 mg, 2.25 mmol) and amine **26** (150 mg, 0.45 mmol) as described for compound **25** and purified by flash chromatography (95:5 AcOEt/MeOH) followed by recrystallization in EtOH. Yellow crystalline powder (202 mg, 87%); mp 240–242 °C.  $^1\text{H}$  NMR (300 MHz, DMSO- $d_6$ )  $\delta$  1.79 (s, 3H), 3.77 (s, 3H), 3.89 (d, 1H,  $J = 14.7$  Hz), 5.67 (d, 1H,  $J = 14.7$  Hz), 6.60–6.80 (m, 2H), 6.87 (d, 1H,  $J = 7.5$  Hz), 7.03 (s, 1H), 7.08–7.23 (m, 3H), 7.23–7.65 (m, 10H), 8.60 (s, 1H), 9.45 (s, 1H).  $^{13}\text{C}$  NMR (50 MHz, DMSO- $d_6$ )  $\delta$  17.2, 35.3, 43.2, 100.3, 119.6, 121.4, 123.4, 125.1, 127.2, 127.4, 127.9, 128.3, 128.5, 129.7, 129.9, 130.3, 132.5, 132.8, 135.6, 136.9, 137.1, 138.9, 139.1, 139.8, 140.1, 167.7, 167.9. IR (KBr)  $\nu$  ( $\text{cm}^{-1}$ ) 3303, 3203, 3154, 3014, 2968, 2913, 2863, 1650, 1641, 1611, 1591, 1563, 1539, 1505, 1449, 1386, 1326, 1298, 1268, 1254, 1177, 1136, 1000, 893, 830, 761, 742, 699. HRMS (ES): calcd for  $\text{C}_{32}\text{H}_{28}\text{N}_5\text{O}_2$ , 514.2238; found, 514.2255. RP-HPLC (gradient 1):  $t_{\text{R}}$  22.3 min, purity > 98%. Anal. ( $\text{C}_{32}\text{H}_{27}\text{N}_5\text{O}_2$ ) C, H, N: calcd, 74.84, 5.30, 13.64; found 74.60, 5.49, 13.55.

**Methyl 3-Methyl-4-(3-methyl-1H-pyrazol-1-yl)benzoate (29a).** A solution of methyl 4-fluoro-3-methylbenzoate **28a** (417 mg, 2.48 mmol), 3-methylpyrazole (0.30 mL, 3.72 mmol), and  $\text{K}_2\text{CO}_3$  (686 mg, 4.96 mmol) in dry NMP (3 mL) was heated at 120 °C under argon. As TLC showed incomplete reaction after 5 h, an additional amount of 3-methylpyrazole (0.30 mL, 3.72 mmol) was added and heating was continued for 20 h. The reaction mixture was then poured into water (30 mL) and extracted with AcOEt (2  $\times$  150 mL). The combined organic layers were dried ( $\text{Na}_2\text{SO}_4$ ) and concentrated in vacuo. Flash chromatography (*n*-heptane to 75:25 *n*-heptane/ $\text{Et}_2\text{O}$ ) afforded the title compound as a colorless oil ( $R_{\text{f}} = 0.2$ , 49.2 mg, 9%).  $^1\text{H}$  NMR (200 MHz,  $\text{CDCl}_3$ )  $\delta$  2.37 (s, 3H), 2.38 (s, 3H), 3.93 (s, 3H), 6.25 (d, 1H,  $J = 2.4$  Hz), 7.42 (d, 1H,  $J = 8.3$  Hz), 7.55 (d, 1H,  $J = 2.2$  Hz), 7.93 (m, 1H), 7.99 (m, 1H).  $^{13}\text{C}$  NMR (75 MHz,  $\text{CDCl}_3$ )  $\delta$  13.5, 18.6, 52.2, 106.7, 125.7, 128.0, 129.2, 131.2, 132.8, 132.9, 143.4, 150.2, 166.4. IR (CsI)  $\nu$  ( $\text{cm}^{-1}$ ) 2953, 2928, 2852, 1721, 1610, 1585, 1535, 1505, 1437, 1394, 1364, 1288, 1267, 1248, 1218, 1198, 1130, 1112, 1040, 1012, 980, 949, 843, 788, 770, 716. The isomer methyl 3-methyl-4-(5-methyl-1H-pyrazol-1-yl)benzoate was also isolated as a yellow solid ( $R_{\text{f}} = 0.1$ , 3.7 mg, 1%); mp 58–60 °C.  $^1\text{H}$  NMR (200 MHz,  $\text{CDCl}_3$ )  $\delta$  2.10 (s, 3H), 2.12 (s, 3H), 3.94 (s, 3H), 6.20 (s, 1H), 7.30 (d, 1H,  $J = 8.0$  Hz), 7.60 (d, 1H,  $J = 1.6$  Hz), 7.96 (m, 1H), 8.02 (m, 1H).  $^{13}\text{C}$  NMR (75 MHz,  $\text{CDCl}_3$ )  $\delta$  11.3, 17.3, 52.3, 105.7, 127.8, 130.7, 132.3, 136.6, 139.46, 139.9, 142.3, 142.4, 166.4. IR (CsI)  $\nu$  ( $\text{cm}^{-1}$ ) 2954, 2924, 2852, 1726, 1613, 1586, 1544, 1509, 1438, 1411, 1391, 1297, 1257, 1201, 1132, 1106, 1018, 976, 923, 786, 773, 724.

**Methyl 2-Chloro-4-(3-methyl-1H-pyrazol-1-yl)benzoate (29b).** Prepared from methyl 2-chloro-4-fluorobenzoate **28b** (1.00 g, 5.30 mmol) and 3-methylpyrazole (0.51 mL, 6.36 mmol) as described for compound **29a** (6 h reflux); white solid (545 mg, 41%);  $R_{\text{f}} = 0.5$  (7:3 *n*-heptane/AcOEt); mp 64–65 °C.  $^1\text{H}$  NMR (200 MHz,  $\text{CDCl}_3$ )  $\delta$  2.38 (s, 3H), 3.94 (s, 3H), 6.31 (d, 1H,  $J = 2.4$  Hz), 7.60 (dd, 1H,  $J = 8.6, 2.2$  Hz), 7.82 (d, 1H,  $J = 2.2$  Hz), 7.86 (d, 1H,  $J = 2.4$  Hz), 7.97 (d, 1H,  $J = 8.6$  Hz).  $^{13}\text{C}$  NMR (50 MHz,  $\text{CDCl}_3$ )  $\delta$  13.7, 52.4, 109.0, 115.6, 120.4, 126.1, 127.5, 133.0, 135.6, 142.8, 152.0, 165.3. IR (KBr)  $\nu$  ( $\text{cm}^{-1}$ ) 3153, 2987, 2947, 2929, 2848, 1730, 1604, 1572, 1541, 1505, 1439, 1395, 1378, 1359, 1310, 1264, 1251, 1226, 1194, 1124, 1088, 1044, 965, 951, 834, 769, 750. Isomer methyl 2-chloro-4-(5-methyl-1H-pyrazol-1-yl)benzoate; cream-colored solid (93 mg, 7%);  $R_{\text{f}} = 0.4$  (7:3 *n*-heptane/AcOEt); mp 80–81 °C.  $^1\text{H}$  NMR (300 MHz,  $\text{CDCl}_3$ )  $\delta$  2.44 (s, 3H), 3.97 (s, 3H), 6.24 (s, 1H), 7.48 (dd, 1H,  $J = 8.4,$

1.9 Hz), 7.62 (s, 1H), 7.67 (d, 1H,  $J = 2.2$  Hz), 7.98 (d, 1H,  $J = 8.4$  Hz).  $^{13}\text{C}$  NMR (75 MHz,  $\text{CDCl}_3$ )  $\delta$  12.8, 52.5, 108.4, 121.7, 126.3, 128.1, 132.2, 134.7, 139.0, 141.0, 143.0, 165.3. IR (KBr)  $\nu$  ( $\text{cm}^{-1}$ ) 3111, 3053, 2989, 2950, 2846, 1733, 1604, 1403, 1261, 1119, 1054, 504.

**3-Methyl-4-(3-methyl-1H-pyrazol-1-yl)benzoic Acid (30a).** A solution of **29a** (137 mg, 0.597 mmol) in a 1:1 6 N HCl/AcOH mixture (2 mL) was refluxed for 6 h and then poured in an ice/water mixture (30 mL) and extracted with  $\text{CHCl}_3$  (2  $\times$  50 mL). The combined organic layers were dried ( $\text{Na}_2\text{SO}_4$ ) and concentrated in vacuo to yield the title compound as a white powder (128 mg, 99%); mp 142–144 °C.  $^1\text{H}$  NMR (300 MHz,  $\text{CDCl}_3$ )  $\delta$  2.39 (s, 3H), 2.40 (s, 3H), 6.27 (d, 1H,  $J = 2.2$  Hz), 7.46 (d, 1H,  $J = 8.1$  Hz), 7.57 (d, 1H,  $J = 2.2$  Hz), 8.00 (dd, 1H,  $J = 8.3, 1.7$  Hz), 8.06 (s, 1H), 10.53 (bs, 1H).  $^{13}\text{C}$  NMR (75 MHz,  $\text{CDCl}_3$ )  $\delta$  13.5, 18.7, 106.9, 125.8, 128.5, 128.6, 131.3, 132.9, 133.5, 143.8, 150.4, 170.8. IR (KBr)  $\nu$  ( $\text{cm}^{-1}$ ) 3200–2400, 2986, 2929, 1678, 1610, 1579, 1540, 1508, 1433, 1402, 1367, 1317, 1304, 1284, 1221, 1068, 1041, 952, 926, 911, 834, 771, 754, 577.

**2-Chloro-4-(3-methyl-1H-pyrazol-1-yl)benzoic Acid (30b).** A solution of **29b** (545 mg, 2.17 mmol) in a 1:1 6 N HCl/AcOH mixture (7 mL) was refluxed for 6 h and then poured in an ice/water mixture (50 mL). The precipitate was filtered, washed with water, and dried in vacuo under  $\text{P}_2\text{O}_5$  to yield the title compound as a white powder (493 mg, 99%); mp 166–168 °C (sublimation).  $^1\text{H}$  NMR (300 MHz, DMSO- $d_6$ )  $\delta$  2.26 (s, 3H), 6.40 (d, 1H,  $J = 2.5$  Hz), 7.80–8.00 (m, 3H), 8.53 (d, 1H,  $J = 2.2$  Hz), 13.32 (bs, 1H).  $^{13}\text{C}$  NMR (75 MHz, DMSO- $d_6$ )  $\delta$  13.4, 109.0, 115.8, 119.0, 126.9, 129.1, 132.8, 133.6, 142.1, 151.1, 165.8. IR (KBr)  $\nu$  ( $\text{cm}^{-1}$ ) 3146, 3081, 2952, 2800–2300, 1731, 1602, 1538, 1433, 1369, 1298, 1252, 1123, 1047, 965, 831.

**1-Methyl-5-[3-methyl-4-(3-methyl-1H-pyrazol-1-yl)benzoyl]-1,4,5,10-tetrahydropyrazolo[3,4-*b*][1,5]benzodiazepine (31a).** To a stirred solution of **30a** (114 mg, 0.530 mmol) in dry DCM (3 mL) at 0 °C under argon were added successively dry NMP (3 drops) and  $\text{SOCl}_2$  (0.10 mL, 1.325 mmol). The resulting reaction mixture was stirred at rt overnight. The solvent was removed in vacuo, and the resulting residue was dissolved in dry THF. The solvent was removed in vacuo, and the resulting residue was dried under high vacuum for 1 h. Amide coupling was then performed starting from the acyl chloride and amine **7** (116.7 mg, 0.583 mmol) as described for compound **21a** (stirring at rt for 3 days, 10% citric acid wash instead of 1 N HCl, flash chromatography in 98:2 DCM/MeOH); cream-colored foam (113 mg, 53%); mp 140–142 °C.  $^1\text{H}$  NMR (300 MHz,  $\text{CDCl}_3$ )  $\delta$  2.15 (s, 3H), 2.32 (s, 3H), 3.84 (s, 3H), 3.98 (d, 1H,  $J = 14.6$  Hz), 5.92 (d, 1H,  $J = 14.6$  Hz), 6.17 (s, 1H), 6.72 (s, 2H), 6.91 (bs, 1H), 6.95–7.15 (m, 4H), 7.30 (s, 2H), 7.39 (s, 1H).  $^{13}\text{C}$  NMR (50 MHz,  $\text{CDCl}_3$ )  $\delta$  13.5, 18.3, 35.0, 43.3, 101.7, 106.4, 119.4, 122.9, 124.9, 126.1, 128.7, 130.6, 131.2, 131.4, 132.6, 132.7, 135.1, 135.5, 137.7, 140.2, 140.8, 149.8, 168.6. IR (KBr)  $\nu$  ( $\text{cm}^{-1}$ ) 3289, 3137, 3064, 2958, 2927, 2872, 1634, 1606, 1561, 1532, 1504, 1447, 1397, 1380, 1322, 1295, 1251, 1178, 1136, 1040, 992, 951, 837, 815, 758, 733. HRMS (ES): calcd for  $\text{C}_{23}\text{H}_{23}\text{N}_6\text{O}$ , 399.1928; found, 399.1922. RP-HPLC (gradient 1, flow rate: 1 mL/min):  $t_{\text{R}}$  19.6 min, purity > 98%.

**5-[2-Chloro-4-(3-methyl-1H-pyrazol-1-yl)benzoyl]-1-methyl-1,4,5,10-tetrahydro pyrazolo[3,4-*b*][1,5]benzodiazepine (31b).** Prepared from acid **30b** (280 mg, 1.18 mmol) and amine **7** (182 mg, 0.91 mmol) as described for compound **31a**, but the reaction mixture was irradiated under microwaves at 80 °C (2 bar) for 8 min; beige powder (309 mg, 81%); two isomers present in 3:1 proportions; mp 176–178 °C (from EtOH).  $^1\text{H}$  NMR (300 MHz,  $\text{CDCl}_3$ )  $\delta$  2.32 (s, 2.27H), 2.39 (s, 0.73H), 3.76 (s, 3H), 4.05 (d, 1H,  $J = 14.3$  Hz), 5.87 (d, 1H,  $J = 14.4$  Hz), 6.22 (d, 0.9H,  $J = 2.2$  Hz), 6.32 (s, 1H), 6.68 (t, 1H,  $J = 7.5$  Hz), 6.86 (d, 1H,  $J = 7.8$  Hz), 6.90–7.20 (m, 3H), 7.20–7.45 (m, 2H), 7.58 (d, 0.9H,  $J = 1.9$  Hz), 7.70 (d, 0.9H,  $J = 2.2$  Hz), 7.83 (d, 0.2H,  $J = 2.2$  Hz), 7.91 (app bs, 0.2H).  $^{13}\text{C}$  NMR (75 MHz,  $\text{CDCl}_3$ )  $\delta$  13.65, 34.80, 42.98, 100.96, 108.4, 115.7, 119.1, 119.2,

122.3, 127.4, 128.5, 129.0, 129.9, 132.2, 133.4, 136.4, 138.1, 139.1, 140.6, 151.4, 166.6. IR (ATR)  $\nu$  (cm<sup>-1</sup>) 3304, 2929, 1627, 1603, 1563, 1558, 1537, 1504, 1448, 1410, 1398, 1360, 1323, 1301, 1254, 1246, 1229, 1151, 1049, 956, 947, 838, 827, 788, 767, 756, 731, 718, 702, 522, 440. HRMS (ES): calcd for C<sub>22</sub>H<sub>20</sub>ClN<sub>6</sub>O, 419.1382; found, 419.1376. RP-HPLC (gradient 2): *t*<sub>R</sub> 18.7 min, purity 97.2% (254 nm).

**Biology: Material and Methods.** AVP and OT were purchased from Bachem or Novabiochem, [<sup>3</sup>H]AVP from Amersham or PerkinElmer Life and Analytical Sciences, BSA from Sigma and Ro-20-1724 (4-(3-butoxy-4-methoxyphenyl)methyl-2-imidazolide) from Calbiochem. Synthesized compounds were initially dissolved in DMSO at 10 or 1  $\mu$ M and then diluted to the desired concentration with the assay buffer.

**Cell Culture.** The CHO cell lines, which stably express the human vasopressin V<sub>1a</sub>, V<sub>2</sub>, or oxytocin receptors, were maintained in culture in Dulbecco's modified Eagle's medium (D-MEM) supplemented with 10% fetal calf serum, one dose of nonessential amino acids, 100 units/mL penicillin, and 100  $\mu$ g/mL streptomycin in an atmosphere of 95% air and 5% CO<sub>2</sub> at 37 °C.

**Membrane Preparations.** To increase the level of expression of some receptors (OT-R, V<sub>1a</sub>-R), the cells were treated overnight with 5 mM sodium butyrate.<sup>35,55</sup> As already published, this treatment does not modify the pharmacological properties of the receptors. The membranes were prepared as already described.<sup>34–36,50,55</sup> Briefly, culture dishes of CHO cells expressing the human vasopressin V<sub>1a</sub>, V<sub>2</sub>, or oxytocin receptors were washed twice in phosphate-buffered saline without Ca<sup>2+</sup> and Mg<sup>2+</sup>, and cold lysis buffer (15 mM Tris-HCl, 2 mM MgCl<sub>2</sub>, 0.3 mM EDTA, pH 7.4) was added. Cells were scraped with a rubber, Polytron-homogenized, and centrifuged at 800g for 7 min at 4 °C. Supernatants were recovered and centrifuged at 44000g for 25 min at 4 °C. Pellets were resuspended in a suspension medium (50 mM Tris-HCl, 5 mM MgCl<sub>2</sub>, pH 7.4) and centrifuged at 44000g for 25 min at 4 °C. Pellets were resuspended in an appropriate volume of the same buffer, and the protein content was determined by the Bradford method (Bio-Rad) using BSA as the standard. Aliquots of membranes were used immediately for binding assays or stored at -80 °C.

**Radioligand Binding Assays.** Binding assays were performed at 30 °C using [<sup>3</sup>H]AVP as the radioligand and CHO cell-membrane proteins (10–15  $\mu$ g for V<sub>1a</sub> and OT receptors, 5  $\mu$ g for V<sub>2</sub> receptor), as previously described.<sup>34–36,50,55</sup> Briefly, membranes of CHO cells stably expressing human vasopressin V<sub>1a</sub>, V<sub>2</sub>, or oxytocin receptors were incubated for 30 min at 30 °C in the binding buffer (50 mM Tris-HCl, 5 mM MgCl<sub>2</sub>, 1 mg/mL BSA, pH 7.4) with the radiolabeled and displacing ligands. The affinities (*K*<sub>d</sub>) of [<sup>3</sup>H]AVP for the human vasopressin V<sub>1a</sub>, V<sub>2</sub>, and oxytocin receptors have already been described earlier in saturation experiments, respectively *K*<sub>d</sub> = (0.70 ± 0.17) nM, (1.36 ± 0.45) nM, and (1.36 ± 1.00) nM.<sup>30,55</sup> The affinities (*K*<sub>i</sub>) of the unlabeled ligands were determined by competition experiments using [<sup>3</sup>H]AVP (1–2 nM) and varying the concentrations of the displacing ligands from 0.1 pM to 100  $\mu$ M (without exceeding a 4% final concentration in DMSO). Nonspecific binding was determined by adding an excess of AVP (10  $\mu$ M). Bound and free radioactivity were separated by filtration on a Brandel apparatus over Whatman GF/C filters presoaked in a 10 mg/mL BSA solution for 3–4 h. Radioactivity on the filters was counted on a  $\beta$ -counter Tricarb 2100TR (Packard). The ligand binding data were analyzed by nonlinear least-squares regression using the computer program Kell Radlig. The inhibition constants (*K*<sub>i</sub>) for unlabeled ligands were calculated according to the Cheng and Prusoff equation:  $K_i = IC_{50}/(1 + [L^*]/K_d)$ , where IC<sub>50</sub> is the concentration of unlabeled ligand leading to half-maximal inhibition of specific binding, [L\*] is the concentration of the radioligand present in the assay, and *K*<sub>d</sub> is its affinity for the receptor studied. The given *K*<sub>i</sub> values are expressed as the mean ± SEM of at least three independent experiments, each performed in triplicate, unless otherwise specified.

**Functional Assays.** The functional agonist and competitive antagonist properties of each ligand were determined for the human vasopressin and oxytocin receptors subtypes stably expressed in CHO cells. The accumulation of *myo*-inositol 1-phosphate (V<sub>1a</sub> and OT receptors) was determined by the IP-One assay, and the accumulation of cAMP (V<sub>2</sub> receptor) was determined by the cAMP *dynamic 2* assay, both kindly provided by Cisbio International. Briefly, CHO cells stably expressing the human vasopressin V<sub>1a</sub>, V<sub>2</sub>, or oxytocin receptors were seeded (at 80–90% confluence) at a density of 80000 cells/well for V<sub>1a</sub> and OT receptors, and 1000 cells/well for V<sub>2</sub> receptor, in 96-well culture plates (Greiner) in their culture medium in an atmosphere of 95% air and 5% CO<sub>2</sub> at 37 °C overnight. After removal of the culture medium, ligands in the stimulation buffer (already furnished in the IP-One kit; D-MEM supplemented with 0.1 mM of the phosphodiesterases inhibitor Ro-20-1724 and 1 mg/mL BSA for the cAMP assay) were added in increasing final concentrations ranging from 10 fM to 100  $\mu$ M (without exceeding a 1% final concentration in DMSO). To test the agonist effect, cells were incubated with the ligands for 30 min (37 °C + 5% CO<sub>2</sub>), the positive control used being 1  $\mu$ M AVP for V<sub>1a</sub>-R, 0.1  $\mu$ M AVP for V<sub>2</sub>-R, and 1  $\mu$ M OT for OT-R. To test the competitive antagonist effect, cells were preincubated with the ligands for 10 min (37 °C + 5% CO<sub>2</sub>) and then stimulated by the corresponding endogenous agonist (2 nM AVP for V<sub>1a</sub>-R, 1 nM AVP for V<sub>2</sub>-R, and 50 nM OT for OT-R) and incubated for 30 min (37 °C + 5% CO<sub>2</sub>). The cells were lysed and incubated at rt with the IP<sub>1</sub>-d2 and anti-IP<sub>1</sub>-cryptate conjugates (IP-One), or cAMP-d2 and anti-cAMP-cryptate conjugates (cAMP *dynamic 2*). After 1–2 h incubation, fluorescence emissions were measured both at 620 nm and at 665 nm on a RubyStar fluorometer (BMG Labtechnologies) equipped with a nitrogen laser as excitation source (337 nm). A 400  $\mu$ s reading was measured after a 50  $\mu$ s delay to eliminate the short-lived fluorescence background from the specific signal. The fluorescence intensities measured at 620 nm and at 665 nm correspond to the total europium cryptate emission and to the FRET signal, respectively. The specific signal was calculated using the following equation:  $\Delta F = (R - R_{neg})/R_{neg}$ . *R* is the ratio (fluorescence 665 nm/fluorescence 620 nm) × 100 calculated in wells incubated with both donor- and acceptor-labeled antibodies, whereas *R*<sub>neg</sub> is the same ratio for the negative control. The functional data were analyzed by nonlinear regression using GraphPad Prism. For the agonist properties, concentrations of ligands leading to half-maximal IP<sub>1</sub> or cAMP accumulation (EC<sub>50</sub> or activation constant *K*<sub>act</sub>) were calculated from the sigmoidal dose–response curves, and the maximal responses induced by ligands (*E*<sub>max</sub>) are expressed as percentages of maximal stimulation of IP<sub>1</sub> or cAMP accumulation by the corresponding endogenous agonist. For the antagonist properties, concentrations of ligands leading to half-maximal inhibition (IC<sub>50</sub>) of IP<sub>1</sub> or cAMP accumulation were calculated from the inversed sigmoidal dose–response curve. The inactivation constants (*K*<sub>inact</sub>) were calculated as:  $K_{inact} = IC_{50}/(1 + [ago]/K_{act})$ , where [ago] is the concentration of the endogenous agonist present in the assay ([AVP] = 2 nM for V<sub>1a</sub>-R, [AVP] = 1 nM for V<sub>2</sub>-R, and [OT] = 50 nM for OT-R), and *K*<sub>act</sub> is the concentration of this agonist inducing half-maximal stimulation of IP<sub>1</sub> or cAMP accumulation (*K*<sub>act</sub> (AVP) = (1.20 ± 0.33) nM for V<sub>1a</sub>-R, *K*<sub>act</sub> (AVP) = (0.25 ± 0.07) nM for V<sub>2</sub>-R, and *K*<sub>act</sub> (OT) = (10.6 ± 0.3) nM for OT-R). Results are expressed as the mean ± SEM of at least three independent experiments, each performed in triplicate, unless otherwise specified.

**Molecular Modeling.** The protocol used for molecular modeling studies was as published recently by our group.<sup>37</sup> Very briefly, the residue numbering proposed by Ballesteros and Weinstein<sup>94</sup> was used throughout this manuscript. It allows an unambiguous comparison of TM residues for any class A GPCR by assigning position 50 to a fully conserved amino acid at each TM and numbering other amino acids according to this reference residue. Residue x.y is thus the amino acid describing

position y of TMx. For purposes of clarification, amino acids from the peptide ligands will be labeled using a three-letter code, whereas receptor residues will be labeled using a single-letter code.

The amino acid sequences of human OT receptor was retrieved from the Swiss-Prot database and aligned to the sequence of bovine rhodopsin using the in-house developed GPCRmod program<sup>95</sup> focusing on transmembrane (TM) domains only. The alignment of the amino and carboxy-terminal domains as well as of the intra- and extracellular loops was realized using ClustalW.<sup>96</sup> Modeling the AVP-bound conformation of human V<sub>1a</sub> and V<sub>1b</sub> receptors 3-D ground-state models of human V<sub>1a</sub> and V<sub>1b</sub> receptors have recently been reported by our group.<sup>37,55,97,98</sup> To achieve an agonist-bound model from an antagonist-bound model, we followed a five-step protocol as proposed by Bissantz et al.<sup>97</sup> It should be observed that the starting conformation of OT was modeled from the X-ray structure of neurophysin-bound OT.<sup>39</sup> Compound **1** was built starting from the X-ray structure of its truncated analogue **12c**, and then it was fully optimized with HF/6-31\* level using geometry optimization with Gaussian 03.<sup>40</sup> OT and compound **1** were docked to this preliminary model using the Gold 3.0 program.<sup>38</sup> For each of the 10 independent genetic algorithm (GA) runs, a maximum number of 1000 GA operations was performed on a single population of 50 individuals. Operator weights for crossover, mutation, and migration were set to 100, 100, and 0, respectively. To allow poor nonbonded contacts at the start of each GA run, the maximum distance between hydrogen donors and fitting points was set to 5 Å, and nonbonded van der Waals energies were cut off at a value equal to *kij* (well depth of the van der Waals energy for the atom pair *i,j*). To further speed up the calculation, the GA docking was stopped when the top three solutions were within 1.5 Å rmsd. If this criterion is met, we can assume that these top solutions represent a reproducible pose for the ligand.

**Acknowledgment.** Warm thanks are due to Dr. Hadjila Chabane for the preparation of compound **15** and for her constant connection to the project, and to Dr. Dominique Bonnet and Didier Rognan for their scientific support. This work was supported by the Ministère de la Recherche for fundings to MCF and by the European Commission for the Marie-Curie fellowship to J.R. (HPMF-CT-2002-02141). L.B. was supported by grants from the French Agence Nationale de la Recherche (ANR-06-PCVI-0021-03). This work was possible due to the Plateforme Pharmacologie-Criblage-Interactome of the Institut Fédératif de Recherche no. 3 in Montpellier. This work was supported by grants from CNRS, INSERM, Université de Strasbourg, and Université Montpellier 1 and 2. We thank Pascale Buisine and Patrick Werhung (IFR85) for MS analyses and Cyril Anthaume for NMR analyses.

**Supporting Information Available:** Proposed binding mode of oxytocin to human oxytocin receptor and HPLC tracings for target compounds. This material is available free of charge via the Internet at <http://pubs.acs.org>.

## References

- Carter, C. S. Neuroendocrine perspectives on social attachment and love. *Psychoneuroendocrinology* **1998**, *23*, 779–818.
- Insel, T. R.; Young, L. J. The neurobiology of attachment. *Nat. Rev. Neurosci.* **2001**, *2*, 129–136.
- Komisaruk, B. R.; Whipple, B. Love as sensory stimulation: physiological consequences of its deprivation and expression. *Psychoneuroendocrinology* **1998**, *23*, 927–944.
- Zeki, S. The neurobiology of love. *FEBS Lett.* **2007**, *581*, 2575–2579.
- Debiec, J. From affiliative behaviours to romantic feelings: a role of neuropeptides. *FEBS Lett.* **2007**, *581*, 2580–2586.
- Porges, S. W. Love: an emergent property of the mammalian autonomic nervous system. *Psychoneuroendocrinology* **1998**, *23*, 837–861.
- Zak, P. J.; Kurzban, R.; Matzner, W. T. The neurobiology of trust. *Ann. N. Y. Acad. Sci.* **2004**, *1032*, 224–227.
- Zak, P. J.; Kurzban, R.; Matzner, W. T. Oxytocin is associated with human trustworthiness. *Horm. Behav.* **2005**, *48*, 522–527.
- Kosfeld, M.; Heinrichs, M.; Zak, P. J.; Fischbacher, U.; Fehr, E. Oxytocin increases trust in humans. *Nature* **2005**, *435*, 673–676.
- Heinrichs, M.; Baumgartner, T.; Kirschbaum, C.; Ehlert, U. Social support and oxytocin interact to suppress cortisol and subjective responses to psychosocial stress. *Biol. Psychiatry* **2003**, *54*, 1389–1398.
- Uvnäs-Moberg, K. Oxytocin may mediate the benefits of positive social interaction and emotions. *Psychoneuroendocrinology* **1998**, *23*, 819–835.
- DeVries, A. C.; Glasper, E. R.; Detillion, C. E. Social modulation of stress responses. *Physiol. Behav.* **2003**, *79*, 339–407.
- Insel, T. R.; O'Brien, D. J.; Leckman, J. F. Oxytocin, vasopressin, and autism: is there a connection? *Biol. Psychiatry* **1999**, *45*, 145–157.
- Kim, S. J.; Young, L. J.; Gonen, D.; Veenstra-VanderWeele, J.; Courchesne, R.; Courchesne, E.; Lord, C.; Leventhal, B. L.; Cook, E. H., Jr.; Insel, T. R. Transmission disequilibrium testing of arginine vasopressin receptor 1A (AVPR1A) polymorphisms in autism. *Mol. Psychiatry* **2002**, *7*, 503–507.
- Wu, S.; Jia, M.; Ruan, Y.; Liu, J.; Guo, Y.; Shuang, M.; Gong, X.; Zhang, Y.; Yang, X.; Zhang, D. Positive association of the oxytocin receptor gene (OXTR) with autism in the Chinese Han population. *Biol. Psychiatry* **2005**, *58*, 74–77.
- Jacob, S.; Brune, C. W.; Carter, C. S.; Leventhal, B. L.; Lord, C.; Cook, E. H., Jr. Association of the oxytocin receptor gene (OXTR) in Caucasian children and adolescents with autism. *Neurosci. Lett.* **2007**, *417*, 6–9.
- Modahl, C.; Green, L.; Fein, D.; Morris, M.; Waterhouse, L.; Feinstein, C.; Levin, H. Plasma oxytocin levels in autistic children. *Biol. Psychiatry* **1998**, *43*, 270–277.
- Green, L.; Fein, D.; Modahl, C.; Feinstein, C.; Waterhouse, L.; Morris, M. Oxytocin and autistic disorder: alterations in peptide forms. *Biol. Psychiatry* **2001**, *50*, 609–613.
- Hollander, E.; Novotny, S.; Hanratty, M.; Yaffe, R.; DeCaria, C. M.; Aronowitz, B. R.; Mosovich, S. Oxytocin infusion reduces repetitive behaviors in adults with autistic and Asperger's disorders. *Neuropsychopharmacology* **2003**, *28*, 193–198.
- Hollander, E.; Bartz, J.; Chaplin, W.; Phillips, A.; Sumner, J.; Soorya, L.; Anagnostou, E.; Wasserman, S. Oxytocin increases retention of social cognition in autism. *Biol. Psychiatry* **2007**, *61*, 498–503.
- Vassart, G. Non-peptide arginine-vasopressin antagonists: the vaptans. *Lancet* **2008**, *371*, 1624–1632.
- Manning, M.; Stoev, S.; Chini, B.; Durroux, T.; Mouillac, B.; Guillon, G. Peptide and non-peptide agonists and antagonists for the vasopressin and oxytocin V<sub>1a</sub>, V<sub>1b</sub>, V<sub>2</sub> and OT receptors: research tools and potential therapeutic agents. *Prog. Brain Res.* **2008**, *170*, 473–512.
- Ashworth, D. M.; Batt, A. R.; Baxter, A. J.; Broqua, P.; Haigh, R. M.; Hudson, P.; Heeney, C. M. S.; Laporte, R.; Penson, A.; Pitt, G. R. W.; Robson, P. A.; Rooper, D. P.; Tartar, A. L.; Yea, C. M.; Roe, M. B. Nonpeptide oxytocin agonists. *Drugs Future* **2006**, *31*, 345–353.
- Pitt, G. R. W.; Batt, A. R.; Haigh, R. M.; Penson, A. M.; Robson, P. A.; Rooper, D. P.; Tartar, A. L.; Trim, J. E.; Yea, C. M.; Roe, M. B. Non-peptide oxytocin agonists. *Bioorg. Med. Chem. Lett.* **2004**, *14*, 4585–4589.
- Pardridge, W. M. Blood–brain barrier delivery. *Drug Discovery Today* **2007**, *12*, 54–61.
- Matsuhisa, A.; Tanaka, A.; Kikuchi, K.; Shimada, Y.; Yatsu, T.; Yanagisawa, I. Nonpeptide arginine vasopressin antagonists for both V<sub>1a</sub> and V<sub>2</sub> receptors: synthesis and pharmacological properties of 2-phenyl-4'-[(2,3,4,5-tetrahydro-1H-1-benzazepin-1-yl)-carbonyl]benzanilide derivatives. *Chem. Pharm. Bull.* **1997**, *45*, 1870–1874.
- Caggiano, T. J. WAY-VNA-932. *Drugs Future* **2002**, *27*, 248–253.
- Williams, P. D.; Clineschmidt, B. V.; Erb, J. M.; Freidinger, R. M.; Guidotti, M. T.; Lis, E. V.; Pawluczuk, J. M.; Pettibone, D. J.; Reiss, D. R.; Veber, D. F.; Woyden, C. J. 1-[1-[4-[(N-Acetyl-4-piperidinyl)oxy]-2-methoxybenzoyl]piperidin-4-yl]-4H-3,1-benzoxazin-2(1H)-one (L-371,257): a new, orally bioavailable, non-peptide oxytocin antagonist. *J. Med. Chem.* **1995**, *38*, 4634–4636.
- Pitt, G. R. W.; Roe, M. B.; Rooper, D. P. Oxytocin agonists. Patent WO 03/000692 A3, **2003**.

- (30) Sasatani, S.; Miyazaki, T.; Maruoka, K.; Yamamoto, H. Diisobutylaluminum hydride: a novel reagent for the reduction of oximes. *Tetrahedron Lett.* **1983**, *24*, 4711–4712.
- (31) Artico, M.; De Martino, G.; Filacchioni, G.; Giuliano, R. Ricerche su sostanze ad attivita' antiblastica. *Il Farmaco—Ed. Sci.* **1969**, *24*, 276–284.
- (32) Bell, I. M.; Erb, J. M.; Freidinger, R. M.; Gallicchio, S. N.; Guare, J. P.; Guidotti, M. T.; Halpin, R. A.; Hobbs, D. W.; Homnick, C. F.; Kuo, M. S.; Lis, E. V.; Mathre, D. J.; Michelson, S. R.; Pawluczyk, J. M.; Pettibone, D. J.; Reiss, D. R.; Vickers, S.; Williams, P. D.; Woyden, C. J. Development of orally active oxytocin antagonists: studies on 1-(1-[4-[1-(2-methyl-1-oxido-pyridin-3-ylmethyl)piperidin-4-yloxy]-2-methoxybenzoyl]piperidin-4-yl)-1,4-dihydrobenzo[*d*][1,3]oxazin-2-one (L-372,662) and related pyridines. *J. Med. Chem.* **1998**, *41*, 2146–2163.
- (33) Kondo, K.; Ogawa, H.; Shinohara, T.; Kurimura, M.; Tanada, Y.; Kan, K.; Yamashita, H.; Nakamura, S.; Hirano, T.; Yamamura, Y.; Mori, T.; Tominaga, M.; Itai, A. Novel design of nonpeptide AVP V<sub>2</sub> receptor agonists: structural requirements for an agonist having 1-(4-aminobenzoyl)-2,3,4,5-tetrahydro-1*H*-1-benzazepine as a template. *J. Med. Chem.* **2000**, *43*, 4388–4397.
- (34) Carnazzi, E.; Aumelas, A.; Phalipou, S.; Mouillac, B.; Guillon, G.; Barberis, C.; Seyer, R. Efficient photoaffinity labeling of the rat V<sub>1a</sub> vasopressin receptor using a linear azidopeptidic antagonist. *Eur. J. Biochem.* **1997**, *247*, 906–913.
- (35) Phalipou, S.; Cotte, N.; Carnazzi, E.; Seyer, R.; Mahé, E.; Jard, S.; Barberis, C.; Mouillac, B. Mapping peptide-binding domains of the human V<sub>1a</sub> vasopressin receptor with a photoactivatable linear peptide antagonist. *J. Biol. Chem.* **1997**, *272*, 26536–26544.
- (36) Phalipou, S.; Seyer, R.; Cotte, N.; Breton, C.; Barberis, C.; Hibert, M.; Mouillac, B. Docking of linear peptide antagonists into the human V<sub>1a</sub> vasopressin receptor: identification of binding domains by photoaffinity labelling. *J. Biol. Chem.* **1999**, *274*, 23316–23327.
- (37) Rodrigo, J.; Pena, A.; Murat, B.; Trueba, M.; Durroux, T.; Guillon, G.; Rognan, D. Mapping the binding site of arginine vasopressin to V<sub>1a</sub> and V<sub>1b</sub> vasopressin receptors. *Mol. Endocrinol.* **2007**, *21*, 512–523.
- (38) Verdonk, M. L.; Cole, J. C.; Hartshorn, M. J.; Murray, C. W.; Taylor, R. D. Improved protein-ligand docking using GOLD. *Proteins* **2003**, *52*, 609–623.
- (39) Rose, J. P.; Wu, C. K.; Hsiao, C. D.; Breslow, E.; Wang, B. C. Crystal structure of the neurophysin–oxytocin complex. *Nat. Struct. Biol.* **1996**, *3*, 163–169.
- (40) Gaussian, Inc., Wallingford CT, **2004**.
- (41) Barberis, C.; Mouillac, B.; Durroux, T. Structural bases of vasopressin/oxytocin function. *J. Endocrinol.* **1998**, *156*, 223–229.
- (42) Hojro, E.; Eich, P.; Gimpl, G.; Fahrenholz, F. Direct identification of an extracellular agonist binding site in the renal V<sub>2</sub> vasopressin receptor. *Biochemistry* **1993**, *32*, 13537–13544.
- (43) Mouillac, B.; Chini, B.; Balestre, M. N.; Elands, J.; Trumpp-Kallmeyer, S.; Hoflack, J.; Hibert, M.; Jard, S.; Barberis, C. The binding site of neuropeptide vasopressin V<sub>1a</sub> receptor: evidence for a major localization within transmembrane regions. *J. Biol. Chem.* **1995**, *270*, 25771–25777.
- (44) Chini, B.; Mouillac, B.; Ala, Y.; Balestre, M. N.; Trumpp-Kallmeyer, S.; Hoflack, J.; Elands, J.; Hibert, M.; Manning, M.; Jard, S.; Barberis, C. Tyr 115 is the key residue for determining agonist selectivity in the V<sub>1a</sub> vasopressin receptor. *EMBO J.* **1995**, *14*, 2176–2182.
- (45) Ufer, E.; Postina, R.; Gorbulev, V.; Fahrenholz, F. An extracellular residue determines the agonist specificity of V<sub>2</sub> vasopressin receptors. *FEBS Lett.* **1995**, *362*, 19–23.
- (46) Chini, B.; Mouillac, B.; Balestre, M. N.; Trumpp-Kallmeyer, S.; Hoflack, J.; Hibert, M.; Andriolo, M.; Pupier, S.; Jard, S.; Barberis, C. Two aromatic residues regulate the response of the human oxytocin receptor to the partial agonist arginine vasopressin. *FEBS Lett.* **1996**, *397*, 201–206.
- (47) Postina, R.; Kojro, E.; Fahrenholz, F. Separate agonist and peptide antagonist binding sites of the oxytocin receptor defined by their transfer into the V<sub>2</sub> vasopressin receptor. *J. Biol. Chem.* **1996**, *271*, 31593–31601.
- (48) Hibert, M.; Hoflack, J.; Trumpp-Kallmeyer, S.; Mouillac, B.; Chini, B.; Mahé, E.; Jard, S.; Manning, M.; Barberis, C. Functional architecture of vasopressin/oxytocin receptors. *J. Recept. Signal Transduction Res.* **1999**, *19*, 589–596.
- (49) Cotte, N.; Balestre, M. N.; Aumelas, A.; Mahé, E.; Phalipou, S.; Morin, D.; Hibert, M.; Manning, M.; Durroux, T.; Barberis, C.; Mouillac, B. Conserved aromatic residues in the transmembrane region VI of the V<sub>1a</sub> vasopressin receptor differentiate agonist vs antagonist ligand binding. *Eur. J. Biochem.* **2000**, *267*, 4253–4263.
- (50) Breton, C.; Chellil, H.; Kabbaj-Benmansour, M.; Carnazzi, E.; Seyer, R.; Phalipou, S.; Morin, D.; Durroux, T.; Zingg, H.; Barberis, C.; Mouillac, B. Direct identification of human oxytocin receptor-binding domains using a photoactivatable cyclic peptide antagonist: comparison with the human V<sub>1a</sub> vasopressin receptor. *J. Biol. Chem.* **2001**, *276*, 26931–26941.
- (51) Thibonnier, M.; Coles, P.; Thibonnier, A.; Shoham, M. Molecular pharmacology and modelling of vasopressin receptors. *Prog. Brain Res.* **2002**, *139*, 179–196.
- (52) Hawtin, S. R.; Wesley, V. J.; Parslow, R. A.; Simms, J.; Miles, A.; McEwan, K.; Wheatley, M. A single residue (Arg<sup>46</sup>) located within the N-terminus of the V<sub>1a</sub> vasopressin receptor is critical for binding vasopressin but not peptide or nonpeptide antagonists. *Mol. Endocrinol.* **2002**, *16*, 600–609.
- (53) Wesley, V. J.; Hawtin, S. R.; Howard, H. C.; Wheatley, M. Agonist-specific, high-affinity binding epitopes are contributed by an arginine in the N-terminus of the human oxytocin receptor. *Biochemistry* **2002**, *41*, 5086–5092.
- (54) Hawtin, S. R.; Wesley, V. J.; Simms, J.; Parslow, R. A.; Miles, A.; McEwan, K.; Keen, M.; Wheatley, M. An arginyl in the N-terminus of the V<sub>1a</sub> vasopressin receptor is part of the conformational switch controlling activation by agonist. *Eur. J. Biochem.* **2003**, *270*, 4681–4688.
- (55) Tahtaoui, C.; Balestre, M. N.; Klotz, P.; Rognan, D.; Barberis, C.; Mouillac, B.; Hibert, M. Identification of the binding sites of the SR49059 nonpeptide antagonist into the V<sub>1a</sub> vasopressin receptor using sulfhydryl-reactive ligands and cysteine mutants as chemical sensors. *J. Biol. Chem.* **2003**, *278*, 40010–40019.
- (56) Gimpl, G.; Postina, R.; Fahrenholz, F.; Reinheimer, T. Binding domains of the oxytocin receptor for the selective oxytocin receptor antagonist barusiban in comparison to the agonists oxytocin and carbetocin. *Eur. J. Pharmacol.* **2005**, *510*, 9–16.
- (57) Hawtin, S. R.; Simms, J.; Conner, M.; Lawson, Z.; Parslow, R. A.; Trim, J.; Sheppard, A.; Wheatley, M. Charged extracellular residues, conserved throughout a G-protein-coupled receptor family, are required for ligand binding, receptor activation, and cell-surface expression. *J. Biol. Chem.* **2006**, *281*, 38478–38488.
- (58) Macion-Dazard, R.; Callahan, N.; Xu, Z.; Wu, N.; Thibonnier, M.; Shoham, M. Mapping the binding site of six nonpeptide antagonists to the human V<sub>2</sub>-renal vasopressin receptor. *J. Pharmacol. Exp. Ther.* **2006**, *316*, 564–571.
- (59) Conner, M.; Hawtin, S. R.; Simms, J.; Wooten, D.; Lawson, Z.; Conner, A. C.; Parslow, R. A.; Wheatley, M. Systematic analysis of the entire second extracellular loop of the V<sub>1a</sub> vasopressin receptor: key residues, conserved throughout a G-protein-coupled receptor family, identified. *J. Biol. Chem.* **2007**, *282*, 17405–17412.
- (60) Nakamura, S.; Yamamura, Y.; Itoh, S.; Hirano, T.; Tsujimae, K.; Aoyama, M.; Kondo, K.; Ogawa, H.; Shinohara, T.; Kan, K.; Tanada, Y.; Teramoto, S.; Sumida, T.; Nakayama, S.; Sekiguchi, K.; Kambe, T.; Tsujimoto, G.; Mori, T.; Tominaga, M. Characterization of a novel nonpeptide vasopressin V<sub>2</sub>-agonist, OPC-51803, in cells transfected human vasopressin receptor subtypes. *Br. J. Pharmacol.* **2000**, *129*, 1700–1706.
- (61) WAY-141608. *Drug Data Rep.* **2000**, *22*, 520.
- (62) Kondo, K.; Kan, K.; Tanada, Y.; Bando, M.; Shinohara, T.; Kurimura, M.; Ogawa, H.; Nakamura, S.; Hirano, T.; Yamamura, Y.; Kido, M.; Mori, T.; Tominaga, M. Characterization of orally active nonpeptide vasopressin V<sub>2</sub> receptor agonists: synthesis and biological evaluation of both the (5*R*)- and (5*S*)-enantiomers of 2-[1-(2-chloro-4-pyrrolidin-1-yl-benzoyl)-2,3,4,5-tetrahydro-1*H*-1-benzazepin-5-yl]-*N*-isopropylacetamide. *J. Med. Chem.* **2002**, *45*, 3805–3808.
- (63) Failli, A. A.; Shumsky, J. S.; Steffan, R. J.; Caggiano, T. J.; Williams, D. K.; Trybulski, E. J.; Ning, X.; Lock, Y.; Tanikella, T.; Hartmann, D.; Chan, P. S.; Park, C. H. Pyridobenzodiazepines: a novel class of orally active, vasopressin V<sub>2</sub> receptor selective agonists. *Bioorg. Med. Chem. Lett.* **2006**, *16*, 954–959.
- (64) Yamamura, Y.; Ogawa, H.; Chihara, T.; Kondo, K.; Onogawa, T.; Nakamura, S.; Mori, T.; Tominaga, M.; Yabuuchi, Y. OPC-21268, an orally effective, nonpeptide vasopressin V<sub>1</sub> receptor antagonist. *Science* **1991**, *252*, 572–574.
- (65) Ogawa, H.; Yamashita, H.; Kondo, K.; Yamamura, Y.; Miyamoto, H.; Kan, K.; Kitano, K.; Tanaka, M.; Nakaya, K.; Nakamura, S.; Mori, T.; Tominaga, M.; Yabuuchi, Y. Orally active, nonpeptide vasopressin V<sub>2</sub> receptor antagonists: a novel series of 1-[4-(benzoylamino)benzoyl]-2,3,4,5-tetrahydro-1*H*-benzazepines and related compounds. *J. Med. Chem.* **1996**, *39*, 3547–3555.
- (66) Ariens, E. J. A molecular basis for the action of drugs. I. Receptor–theory and structure–effect relations. *Arzneim. Forsch.* **1966**, *16*, 1376–1395.
- (67) Goddard, W. A., III; Abrol, R. 3-Dimensional structures of G-protein-coupled receptors and binding sites of agonists and antagonists. *J. Nutr.* **2007**, *137*, 1528S–1538S, and references cited therein.



- (68) Portoghese, P. S.; Lipkowski, A. W.; Takemori, A. E. Bimorphans as highly selective, potent kappa opioid receptor antagonist. *J. Med. Chem.* **1987**, *30*, 238–239.
- (69) Perlman, S.; Costa-Neto, C. M.; Miyakawa, A. A.; Schambye, H. T.; Hjorth, S. A.; Paiva, A. C. M.; Rivero, R. A.; Greenlee, W. J.; Schwartz, T. W. Dual agonistic and antagonistic property of nonpeptide angiotensin AT1 ligands: susceptibility to receptor mutations. *Mol. Pharmacol.* **1997**, *51*, 301–311.
- (70) Fürst, S.; Hosztafi, S.; Friedmann, T. Structure–activity relationships of synthetic and semisynthetic opioid agonists and antagonists. *Curr. Med. Chem.* **1995**, *1*, 423–440.
- (71) Aquino, C. J.; Armour, D. R.; Berman, J. M.; Birkemo, L. S.; Carr, R. A. E.; Croom, D. K.; Dezube, M.; Dougherty, R. W.; Ervin, G. N.; Grizzle, M. K.; Head, J. E.; Hirst, G. C.; James, M. K.; Johnson, M. F.; Miller, L. J.; Queen, K. L.; Rimele, T. J.; Smith, D. N.; Sugg, E. E. Discovery of 1,5-benzodiazepines with peripheral cholecystokinin (CCK-A) receptor agonist activity. 1. Optimization of the agonist “trigger”. *J. Med. Chem.* **1996**, *39*, 562–569.
- (72) Asano, M.; Hatori, C.; Sawai, H.; Johki, S.; Inamura, N.; Kayakiri, H.; Satoh, S.; Abe, Y.; Inoue, T.; Sawada, Y.; Mizutani, T.; Oku, T.; Nakahara, K. Pharmacological characterization of a nonpeptide bradykinin B2 receptor antagonist, FR165649, and agonist, FR190997. *Br. J. Pharmacol.* **1998**, *124*, 441–446.
- (73) Gouldson, P.; Legoux, P.; Carillon, C.; Delpech, B.; Le Fur, G.; Ferrara, P.; Shire, D. The agonist SR146131 and the antagonist SR27897 occupy different sites on the human CCK<sub>1</sub> receptor. *Eur. J. Pharmacol.* **2000**, *400*, 185–194.
- (74) Escrieut, C.; Gigoux, V.; Archer, E.; Verrier, S.; Maigret, B.; Behrendt, R.; Moroder, L.; Bignon, E.; Silvente-Poirot, S.; Pradayrol, L.; Fourmy, D. The biologically crucial C terminus of cholecystokinin and the non-peptide agonist SR-146,131 share a common binding site in the human CCK1 receptor: evidence for a crucial role of Met-121 in the activation process. *J. Biol. Chem.* **2002**, *277*, 7546–7555.
- (75) Holst, B.; Mokrosinski, J.; Lang, M.; Brandt, E.; Nygaard, R.; Frimurer, T. M.; Beck-Sickinge, A. G.; Schwartz, T. W. Identification of an efficacy switch region in the ghrelin receptor responsible for interchange between agonism and inverse agonism. *J. Biol. Chem.* **2007**, *282*, 15799–15811.
- (76) Buck, E.; Wells, J. A. Disulfide trapping to localize small-molecule agonists and antagonists of a G protein-coupled receptor. *Proc. Natl. Acad. Sci. U.S.A.* **2005**, *102*, 2719–2724.
- (77) Wise, E. L.; Duchesnes, C.; da Fonseca, P. C. A.; Allen, R. A.; Williams, T. J.; Pease, J. E. Small molecule receptor agonists and antagonists of CCR3 provide insight into mechanisms of chemokine receptor activation. *J. Biol. Chem.* **2007**, *282*, 27935–27943.
- (78) Shen, C. P.; Xiao, J. C.; Armstrong, H.; Hagmann, W.; Fong, T. M. F200A substitution in the third transmembrane helix of human cannabinoid CB<sub>1</sub> receptor converts AM2233 from receptor agonist to inverse agonist. *Eur. J. Pharmacol.* **2006**, *531*, 41–46.
- (79) Jensen, P. C.; Nygaard, R.; Thiele, S.; Elder, A.; Zhu, G.; Kolbeck, R.; Ghosh, S.; Schwartz, T. W.; Rosenkilde, M. M. Molecular interaction of a potent nonpeptide agonist with the chemokine receptor CCR8. *Mol. Pharmacol.* **2007**, *72*, 327–340.
- (80) Hadac, E. M.; Dawson, E. S.; Darrow, J. W.; Sugg, E. E.; Lybrand, T. P.; Miller, L. J. Novel benzodiazepine photoaffinity probe stereoselectively labels a site deep within the membrane-spanning domain of the cholecystokinin receptor. *J. Med. Chem.* **2006**, *49*, 850–863.
- (81) Scarselli, M.; Li, B.; Kim, S. K.; Wess, J. Multiple residues in the second extracellular loop are critical for M<sub>3</sub> muscarinic acetylcholine receptor activation. *J. Biol. Chem.* **2007**, *282*, 7385–7396.
- (82) Banères, J. L.; Mesnier, D.; Martin, A.; Joubert, L.; Dumuis, A.; Bockaert, J. Molecular characterization of a purified 5-HT<sub>4</sub> receptor: a structural basis for drug efficacy. *J. Biol. Chem.* **2005**, *280*, 20253–20260.
- (83) Fleck, B. A.; Chen, C.; Yang, W.; Huntley, R.; Markison, S.; Nickolls, S. A.; Foster, A. C.; Hoare, S. R. J. Molecular interactions of nonpeptide agonists and antagonists with the melanocortin-4 receptor. *Biochemistry* **2005**, *44*, 14494–14508.
- (84) Fleck, B. A.; Ling, N.; Chen, C. Substituted NDP-MSH peptides paired with mutant melanocortin-4 receptors demonstrate the role of transmembrane 6 in receptor activation. *Biochemistry* **2007**, *46*, 10473–10483.
- (85) Foucaud, M.; Tikhonova, I. G.; Langer, I.; Escrieut, C.; Dufresne, M.; Seva, C.; Maigret, B.; Fourmy, D. Partial agonism, neutral antagonism, and inverse agonism at the human wild-type and constitutively active cholecystokinin-2 receptors. *Mol. Pharmacol.* **2006**, *69*, 680–690.
- (86) Kim, S. K.; Gao, Z. G.; Van Rompaey, P.; Gross, A. S.; Chen, A.; Van Calenbergh, S.; Jacobson, K. A. Modeling the adenosine receptors: comparison of the binding domains of A<sub>2A</sub> agonists and antagonists. *J. Med. Chem.* **2003**, *46*, 4847–4859.
- (87) Ghanouni, P.; Gryczynski, Z.; Steenhuis, J. J.; Lee, T. W.; Farrens, D. L.; Lakowicz, J. R.; Kobilka, B. K. Functionally different agonists induce distinct conformations in the G protein coupling domain of the  $\beta_2$  adrenergic receptor. *J. Biol. Chem.* **2001**, *276*, 24433–24436.
- (88) Palczewski, K.; Kumasaka, T.; Hori, T.; Behnke, C. A.; Motoshima, H.; Fox, B. A.; Le Trong, I.; Teller, D. C.; Okada, T.; Stenkamp, R. E.; Yamamoto, M.; Miyano, M. Crystal structure of rhodopsin: a G protein-coupled receptor. *Science* **2000**, *289*, 739–745.
- (89) Schwartz, T. W.; Frimurer, T. M.; Holst, B.; Rosenkilde, M. M.; Elling, C. E. Molecular mechanism of 7TM receptor activation—a global toggle switch model. *Annu. Rev. Pharmacol. Toxicol.* **2006**, *46*, 481–519, and references cited therein.
- (90) Durroux, T. Principles: a model for the allosteric interactions between ligand binding sites within a dimeric GPCR. *Trends Pharmacol. Sci.* **2005**, *26*, 376–384.
- (91) Jaakola, V.-P.; Griffith, M.; Hanson, M. A.; Cherezov, V.; Chien, E. Y.; Lane, J.; IJzerman, J. R.; Stevens, A. P. R.C. The 2.6 Ångstrom Crystal Structure of a Human A<sub>2A</sub> Adenosine Receptor Bound to an Antagonist. *Science* **2008**, *322*, 1211–1217.
- (92) Gurrath, M. Peptide-binding, G protein-coupled receptors: new opportunities for drug design. *Curr. Med. Chem.* **2001**, *8*, 1605–1648.
- (93) Blakeney, J. S.; Reid, R. C.; Le, G. T.; Fairlie, D. P. Nonpeptidic ligands for peptide-activated G protein-coupled receptors. *Chem. Rev.* **2007**, *107*, 2960–3041.
- (94) Ballesteros, J. A.; Weinstein, H. Integrated methods for the construction of three dimensional models and computational probing of structure–function relations in G-protein coupled receptors. *Methods Neurosci.* **1995**, *25*, 366–428.
- (95) Bissantz, C.; Logean, A.; Rognan, D. High-throughput modeling of human G-protein coupled receptors: amino acid sequence alignment, three-dimensional model building, and receptor library screening. *J. Chem. Inf. Comput. Sci.* **2004**, *44*, 1162–1176.
- (96) Thompson, J. D.; Higgins, D. G.; Gibson, T. J. CLUSTAL W: improving the sensitivity of progressive multiple sequence alignment through sequence weighting, position-specific gap penalties and weight matrix choice. *Nucleic Acids Res.* **1994**, *22*, 4673–4680.
- (97) Bissantz, C.; Bernard, P.; Hibert, M.; Rognan, D. Protein-based virtual screening of chemical databases. II. Are homology models of G-protein coupled receptors suitable targets? *Proteins* **2003**, *50*, 5–25.
- (98) Derick, S.; Pena, A.; Durroux, T.; Wagnon, J.; Serradeil, C.; Hibert, M.; Rognan, D.; Guillon, G. Key amino acids located within the transmembrane domains 5 and 7 account for the pharmacological specificity of the human V<sub>1b</sub> vasopressin receptor. *Mol. Endocrinol.* **2004**, *18*, 2777–2789.
- (99) SYBYL 7.3; Tripos International, 1699 South Hanley Road, St. Louis, MO, 63144, **2006**.